Evaluation of the Vertical Accuracy of Open Access Digital Elevation Models across Different Physiographic Regions and River Basins of Nepal

Saroj Karki[1*], Suchana Acharya[2] and Ashok Gautam[3]

[1]Ministry of Physical Infrastructure Development, Province-1, Province Government, Nepal
[2]Department of Water Resources and Irrigation (DoWRI), Government of Nepal
[3]Ministry of Physical Infrastructure Development, Karnali Province, Province Government, Nepal

(sarojioe@gmail.com)

ABSTRACT

The vertical accuracy of eight different freely accessible DEMs have been evaluated across different physiographic divisions and the river basins of Nepal. Results revealed that MERIT is superior to other DEMs (RMSE 9m) in the low lying Terai plains of Nepal where the elevation range is lower. In High mountains and High Himalayas having higher elevation range, SRTM90m outperformed all its counterpart. Meanwhile in Siwalik and middle mountains, both SRTM90m and HYDROSHEDS exhibited almost similar RMSE indicating their compatible uses in these regions. Meanwhile, the accuracy assessment across different river basins of Nepal discerned that the accuracy of SRTM90m was above others in larger river basins like Koshi (RMSE 224m), Narayani (RMSE 215m) and Karnali (RMSE 265m) where the range of elevation is greater. In the smaller to medium-sized basins like Kankai, Kamala, Bagmati, West Rapti and Babai, HYDROSHEDS was preferrable along with SRTM90m. Based on different error statistics, the DEMs were ranked in order of their accuracy.

Keywords: Digital Elevation Models, Terai, Chure, Nepal, River basins.

1. INTRODUCTION

Digital Elevation Models (DEMs) that represent the surface elevation are fundamental to any studies that deal with the earth and environmental science (Jing et al. 2014). DEMs are established as a principal spatial dataset for different hydro-environmental and geosciences applications (Schumann et al. 2018; Yamazaki et al. 2017). Topographic data usually in the form

of DEMs are the most important input data in the study of different types of natural hazards (Boreggio et al. 2018). Hydrologic and hydraulic tools entail the terrain data encompassing from the reach to the basin scale. Delineation of catchment or watershed is carried out based on DEMs which is a primary step for any geomorphological and hydrological studies. For instance, popular hydrologic models like Soil and Water Assessment Tool (SWAT) (Winchell et al. 2013), hydraulic models like Rainfall-Runoff-Inundation (RRI) model (Shrestha 2019), LIS-Flood model (Coulthard et al. 2013), etc. all require DEMs or surface elevation as a primary dataset for model set-up and simulation. Precise representation of the terrain is therefore vital for the accurate prediction that closely agrees with the field observations. There are different techniques which can be employed to generate high resolution digital terrain elevation maps. High cost, time and sophisticated technology associated with these techniques renders them difficult, if not impossible, for a large-scale application in a developing country with limited resources. In the context of developing country like Nepal where the priorities that are centered around the basic physical infrastructure and social development are yet to be achieved, mapping and the preparation of high-resolution surface elevation is still far from the reality. Lack of high-resolution topographical dataset is one of the major impediments to conduct research activities across multiple fields in Nepal. A country with diverse landforms and elevation that ranges from below 60m to the highest peak of the world (Mount Everest, at an elevation of 8848 meter above sea level) in a mere 150Km-200Km stretch, the role of precise elevation dataset cannot be overlooked. Schumann et al. (2018) has highlighted the growing need for the high resolution DEMs. The availability of remotely sensed DEMs at varying spatial resolution have, however, largely benefitted a nation like Nepal with lack of precise topography dataset. The problem regarding the requirement of a country-scale high resolution topographic dataset has, to a certain extent, been alleviated by these DEMs, if not completely. The analysis of different hydro-climatic, environmental, geomorphological, etc. issues have been made possible by the availability of multiple open access DEMs. The release of open access DEMs have eased the analysis of global flood hazard at the global scale (Sampson et al. 2016).

In the midst of this, the problem pertaining to the accuracy of these products needs a proper consideration. The assessment of the accuracy of DEMs is, therefore, a crucial step before confirming their viability for any research studies or real field applications across different fields. The availability of multiple DEMs, on one hand, has given greater access to the users but at the same time it has also created a confusion among the users regarding the selection of a particular DEMs for any applications. The DEMs, however, are not free from errors arising from different sources during the observations and hence require prior processing. Several

analysis and application of the freely available DEMs such as the Shuttle Radar Topography Mission (SRTM) or the Advanced Spaceborne Thermal Emission and Reflection Radiometer (ASTER) have found to exhibit considerable error in vertical. Such errors are further aggravated in the regions with diverse topography (Chu & Lindenschmidt 2017; Schumann et al. 2018). Also, in the flat terrain, the topographic features are not well captured. The issue of the DEMs accuracy has been addressed by several researchers. For instance, Pakoksung & Takagi (2016) evaluated the accuracy of six different DEMs and hence applied the correction to minimize the elevation bias. Their study revealed that the Root Mean Square Error (RMSE) value for coarser resolution DEMs are higher than those of fine-resolution DEMs. Pakoksung & Takagi (2020) also studied about the effect of DEMs on the prediction of run-off and inundation. Their analysis revealed SRTM to perform better among ASTER, SRTM, GMTED2010, HYDROSHEDS, and GTOPO30. In another study, Purinton & Bookhagen (2017) validated the accuracy of different satellite-derived DEMs over Central Andean Plateau by comparing with GPS measurements. They found the ASTER to be of the lowest quality except which all other selected DEMs had the vertical accuracy below 4m.

Most of the previous studies, in general, have either evaluated the accuracy at a small region or a single river basin (Mukherjee et al. 2012; Jing et al. 2014; Rawat et al. 2013). Similarly, the accuracy assessment of DEMs in most cases has focused the evaluation at different elevation bands of a river basin or a particular region. This may likely limit the assessment of the inherent ability of the DEMs to accurately represent the diverse topographic features.

Unlike the aforementioned works, this study attempts to investigate the accuracy of eight freely available DEMs across different physiographic regions as well as across major river basins of Nepal. The main goal of our study is to investigate the performance and accuracy of different space-borne DEM products, specifically across different physiographic regions and river basins as explained above. There have been different studies regarding the accuracy assessment of DEMs. However, this is the first assessment of the accuracy of open-source DEMs at a country-scale in Nepal with diverse topography focusing different physiographic divisions and all the major river basins. In the knowledge of the authors, so far, no formal validation of the accuracy has been conducted for the recently released COPERNICUS DEM.

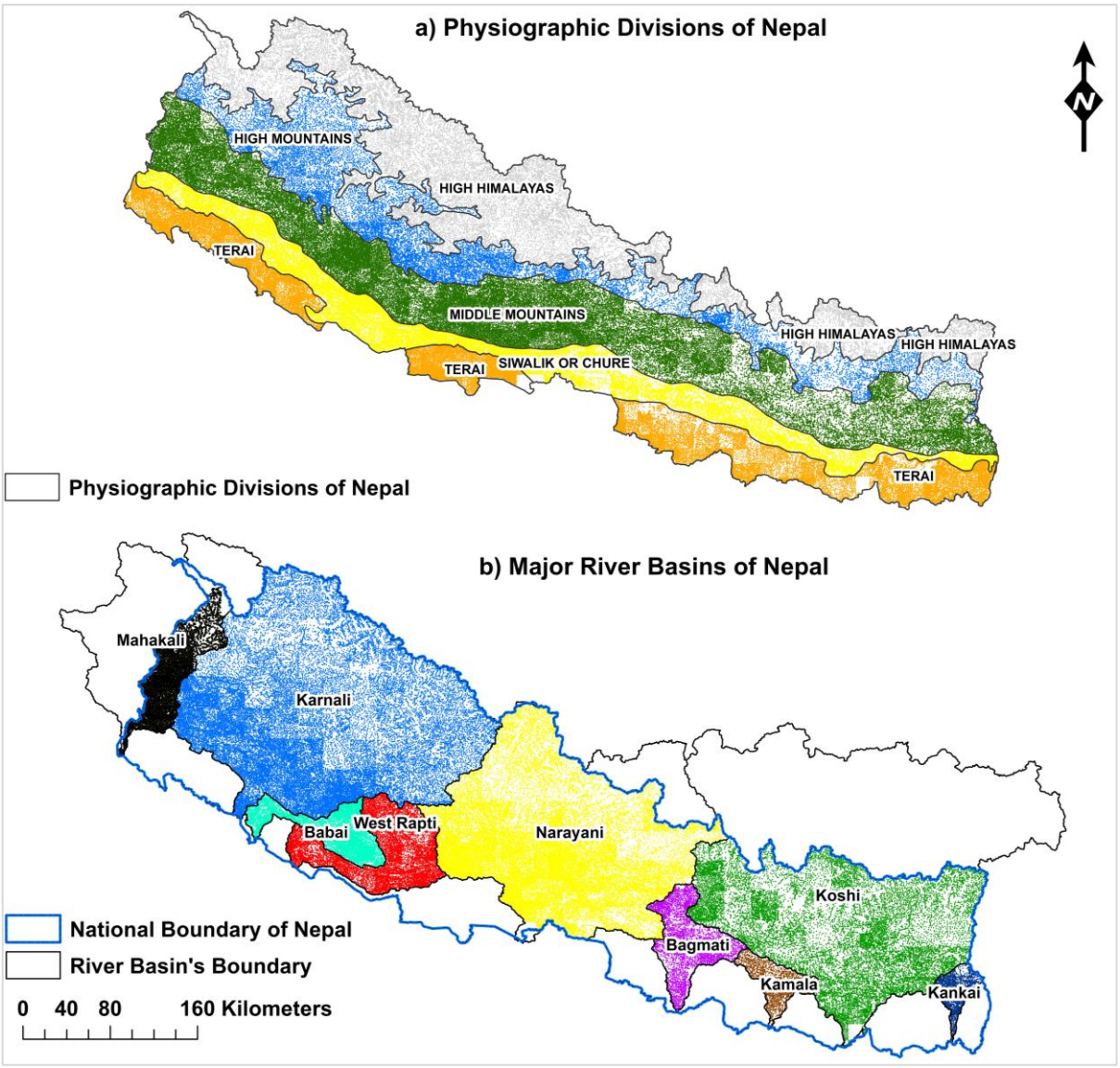

Figure 1. Physiographic divisions and major river basins of Nepal. The color inside the map indicates the reference points which is discussed in subsequent section.

2. STUDY AREA

Nepal is located between two large nations, China in the North while the southern part is bordered by India. Nepal is characterized by a diverse topographical and physiographical landscape with variation in topography across a short North-South stretch. Its altitude ranges from less than 60m in the plains of southern Nepal to over 8000m (Mount Everest, the world's highest summit at elevation of 8,848 masl) in the north, within a short span of about 150 km, where the climate quickly changes from subtropical to arctic conditions (Dhital 2015).

As per the updated map released by the Survey Department in 2020, the area of Nepal is nearly 148,000 square kilometers. Nepal is well-known around the world for the mountain ranges of

111 the Himalayas which includes 8 out of 14 peaks above 8000 meters in the world. The highest
112 peak of the world known as the Mount Everest (Sagarmatha in Nepalese language) also lies
113 within its territory. The world's deepest Kaligandaki gorge also lies here. The country is divided
114 into seven provincial units according to the constitution of Nepal.
115
116 **2.1 Physiographic divisions of Nepal**
117 Topographically, Nepal can be grouped into three distinct ecological divisions, Mountains, Hills
118 and Terai (or Plains), that extend throughout the east-west stretch of the country. Mountains in
119 the north lie at the highest elevation range followed by the Hills and the Terai in the southern
120 part. The broad and widely adopted physiographic units of Nepal, however, comprise of five
121 major divisions viz. high himalayas, high mountains, middle mountains, siwalik (or chure) and
122 the Terai (**Figure 1a**). Each of these physiographic units are characterized by its unique
123 topographical, climatic and vegetational features (Upreti 2001). According to Hagen (1969),
124 the currently adopted five physiographic classes has further been divided into eight
125 physiographic units (Upreti 2001).
126 Terai, the southern unit bordering with India forms the northernmost part of the Indo-Gangetic
127 plain. Along the north, it extends to the foothills of the Siwalik that varies in width
128 approximately between 10km to 50km. Except for about 70Km span of Chitwan valley at the
129 central part and 80Km of the Rapti valley in the west, the Terai region forms continuous belt
130 from the east to the west (**Figure 1a**). At these two locations, the Indo-Nepal border meets the
131 Siwalik. The elevation normally ranges between 100-200m.
132 At the end of the Terai in the north, the abrupt rise in the topography occurs which is the
133 beginning of the Siwalik. The Siwalik hills are often referred as the Chure range in Nepal which
134 occupies about 13% of the total area of Nepal. It forms the southernmost hills of the Himalayas.
135 The elevation generally varies between 200masl to 1000masl and reaches even higher in some
136 locations. Characterized by young and immature geology, these hills are the most fragile in
137 terms of geomorphological features. Numerous gullies and channels dissect these hills which
138 carries significant sediment as a result of the soil erosion and landslides. The rivers originating
139 from these hills are generally ephemeral in nature exhibiting river flow only during the monsoon
140 period. From the view point of conservation, the Siwalik region comes in the top priority be its
141 forest, land resources, rivers, etc.
142 Middle mountains, also known as the Mahabharat range, is the largest physiographic unit of
143 Nepal covering nearly 30% of the total area of the country. The Middle Mountain area

comprises the country's central belt which is composed of networks of ridges and incised valleys (Bricker et al. 2014). High Mountains and High Himalayas which are the source of the major rivers of Nepal comprises almost half of the total area of Nepal. However, due to extreme topographical and climatic features, these regions are one of the least populated area of Nepal.

2.2 River systems of Nepal

The river basins of Nepal can be broadly divided into four major systems, Koshi (or Saptakoshi) in the east, Narayani (or Gandaki) in the central, Karnali in the west and Mahakali in the far west (**Figure 1b**). Out of these, the three Koshi, Narayani and Karnali originate from the Tibetan plateau and cross the Himalayas (Sharma 1987). The flow in these Himalayan rivers is governed by the snowmelt and the glaciers. Apart from these, another group comprise of the rivers originating in the middle mountains whose flow regimes are dictated by the rainfall and the groundwater that prevents the rivers from being completely dry during the low flow period. Kankai, Kamala, Bagmati, West Rapti and Babai are few examples under this group. These rivers have high fluctuations in the discharge between the dry period and the monsoon period. The third group of rivers originate in the Siwalik zone. The flow in these rivers is mostly dependent on monsoon precipitation and their flow level could deplete significantly low during the non-monsoon period. In Nepal, approximately six thousand minor and major streams that span over 40000Km carry annual flow volume of about 1.7bilion cubic meters (DoWRI 2019). The drainage density of Nepal (total river length divided by the total area) is close to 0.3km/square km. The entire area of Nepal forms part of the watershed of Ganges and hence all the Rivers from Nepal eventually join Ganges in India. The Nepalese Rivers contribute as much as 40% flow of Ganges in monsoon and about 70% flow in dry period.

In this study, the four major Himalayan River basins, Koshi, Narayani, Karnali and Mahakali and the five river basins originating in the middle mountains, Kankai, Kamala, Bagmati, West Rapti and Babai are considered (**Figure 1b**). These rivers are characterized by single thread high gradients channels (with frequent meanders) with catchments comprising of steep terrain in the upper reach. The river gradient significantly decreases towards the Terai plain in south. The rivers in the Terai plains are usually braided in nature having multiple channels and often changes the course. The elevation range within each basin are therefore wide that varies in few hundreds to few thousand meters.

3. MATERIALS AND METHODS

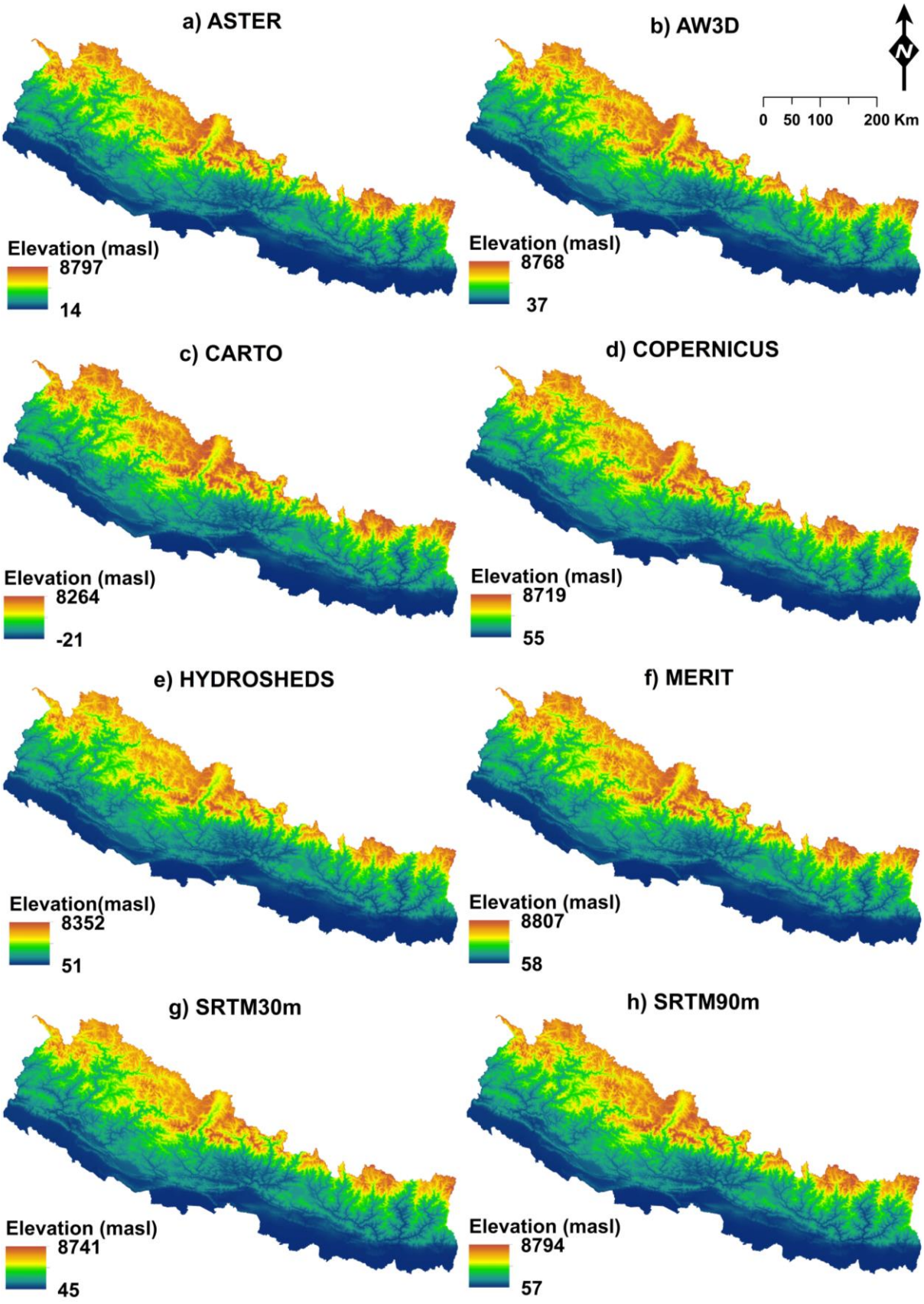

Figure 2. Elevation of Nepal as represented by different DEMs.

3.1 Digital Elevation Models

In this study, eight different freely available DEMs are examined for their vertical accuracy. **Figure 1(a-h)** exhibit the elevation distribution of different DEMs across the country. **Table 1** lists the general information regarding the characteristics of these DEMs including their source, resolution, release year, etc.

Table 1. Characteristics of the DEMs used in this study

DEM	Resolution	Originally Release year	Source	Version used in this sudy	Elevation Range for Nepal (Min/Max) masl
ASTER	30m	2019	METI/NASA	ASTGTMV003	8797/14
AW3D	30m	2016	JAXA	3.1	8768/37
CARTO	30m	2005	ISRO	3-R1	8226/-21
COPERNICUS	30m	2019	ESA	GLO-30	8719/55
HYDROSHEDS	90m	2009	WWF/USGS		8315/60
MERIT	90m	2017	University of Tokyo, Japan	v1.0.3	8807/58
SRTM30m	30m	2014	NASA/USGS	3.0	8741/45
SRTM90m	90m	2003	NASA/USGS	4.1	8794/57

The Advanced Space borne Thermal Emission and Reflection Radiometer (ASTER) Global Digital Elevation Model (GDEM) is the product of joint mission of the United States National Aeronautics and Space Administration (NASA) and the Ministry of Economy, Trade, and Industry (METI) of Japan (Toutin 2008; Gesch et al. 2016) . ASTER DEM has been developed from ASTER scenes dating from March 1, 2000 to November 30, 2013 whose geographic coverage extends from 83° North to 83° South at the horizontal resolution of 30m. ASTER Global Digital Elevation Model V003 has been used in this study which was obtained from the Land Processes Distributed Active Archive Center (LP DAAC) via NASA's Earthdata search (https://search.earthdata.nasa.gov/).

Advanced Land Observing Satellite (ALOS) World 3D-30m (AW3D30) DEM has been released by The Japan Aerospace Exploration Agency (JAXA) in 2016 (Nikolakopoulos 2020). AW3D is a global digital surface model (DSM) dataset with a horizontal resolution of approximately 30 meters (1 arcsec mesh). The dataset is based on the DSM dataset (5-meter mesh version) of the World 3D Topographic Data (JAXA 2017). The AW3D DEM was generated by the "Panchromatic Remote-sensing Instrument for Stereo Mapping (PRISM)" on the "Advanced Land Observing Satellite (ALOS)" which operated from January 2006 to April

2011 (Takaku et al. 2016; Yamazaki et al. 2017). Version 3.1 datasets were acquired from the official website of ALOS Research and Application project. (https://www.eorc.jaxa.jp/ALOS/en/aw3d30/data/index.htm)

The Cartosat-1 Digital Elevation Model (CartoDEM) is a national DEM developed by the Indian Space Research Organization (ISRO) which is derived from the Cartosat-1 stereo payload launched in May 2005 (Mukherjee et al. 2012). For this study, CartoDEM Version-3R1 was downloaded from the bhuvan, Indian geo-platform of ISRO (https://bhuvan-app3.nrsc.gov.in/data/). The data for Nepal is available at the horizontal resolution of 30m.

The Copernicus DEM has been derived from the WorldDEM data which is based on the radar satellite data acquired during the TanDEM-X Mission between 2010-2015, funded by a Public Private Partnership between the German State, represented by the German Aerospace Centre (DLR) and Airbus Defence and Space (Leister-Taylor 2020). The Copernicus DEM is provided in 3 different forms viz. EEA-10, GLO-30 and GLO-90. In the current study, GLO-30 available at 30m horizontal resolution was acquired from the European Space Agency Copernicus website (https://panda.copernicus.eu/web/cds-catalogue/panda).

HydroSHEDS (Hydrological data and maps based on SHuttle Elevation Derivatives at multiple Scales) DEM is derived primarily from elevation data of the Shuttle Radar Topography Mission (SRTM) at 3 arc-second (90m) resolution by hydrological conditioning using a sequence of automated procedures (Lehner et al. 2013; Yan et al. 2019). HydroSHEDS data can for this study was downloaded from https://www.hydrosheds.org/

The MERIT DEM, regarded as one of the most accurate global DEMs, was developed by the group of researchers from the University of Tokyo, Japan. It removed characteristic errors found in these products that included: stripe noise, absolute bias, tree height bias and speckle noise from the existing spaceborne DEMs (SRTM3 v2.1 and AW3D-30m v1) (Yamazaki et al. 2019; Amatulli et al. 2020). It is available at a 3sec resolution (~90m at the equator) and the spatial coverage includes land areas between 90N-60S, referenced to EGM96 geoid (Yamazaki et al. 2017). Merit DEM can be acquired via http://hydro.iis.u-tokyo.ac.jp/~yamadai/MERIT_DEM/

Shuttle Radar Topography Mission (SRTM), a joint mission of National Imagery and Mapping Agency (NIMA) and NASA produced one of the first global DEMs that was first released with a spatial resolution of 3 arc-second (Bhang et al. 2007; Farr et al. 2007; SRTM 2015). SRTM consisted of a specially modified radar system that flew onboard the Space Shuttle Endeavour during an 11-day mission between February 11-22, 2000 (Ling et al. 2005). In 2014, its 1 arc-s global digital elevation model (~30 m) was released. Most parts of the world have been covered

by this data set, ranging from 54°S to 60°N latitude, except for the Middle East and North Africa, which was completed in August 2015 (Nadi et al. 2020). The updated 30m DEM has been released recently to include coverage over Asia and Australia (NASA 2013). The data were downloaded from the LP DAAC via NASA's Earthdata search (https://search.earthdata.nasa.gov/).

3.2 Reference Elevation data

The assessment of the accuracy of DEM requires reference elevation data which are based on the ground observation having higher reliability than the DEM elevations (Pakoksung & Takagi 2016). To this end, we acquired the spot elevation (surveyed elevation point marked from the DoS Toposheet) dataset of more than 120000 points covering the whole country from the Department of Survey (DoS), Nepal. DoS is the national mapping agency of Nepal that is primarily responsible for the surveying, mapping, geoinformation science and earth observation (DoS 2021; Baral 2006). Spot elevation are the digital point data of elevation point locations of Nepal which are based on the Topographic Zonal Map of 250000 scale published by DoS, Nepal in 1988. During the period between 1992 to 2001, DoS updated the old data with a completely new series of topographic base maps replacing the old one inch to one-mile maps. These maps were produced at a scale of 1:25,000 for the terai and the middle mountains; and at a scale of 1:50,000 for the high mountains and Himalayas (Chhatkuli 2003). The spatial distribution of spot elevation point data at the physiographic level and the river basin level is depicted in **Figure 1a** and **b**. The details on these datasets at each physiographic region and the river basin level are listed in **Table 2** and **3** respectively.

Table 2. Details on the data points across the physiographic units.

Physiographic Divisions	Area (Sq. Km.)	Percentage of area occupied	No. of Spot elevations points	Density of points	Elevation Range (Min/Max) masl
Terai	20217	14	22533	1.115	59/721
Siwalik (or Chure)	18976	13	21078	1.111	92/1972
Middle Mountains	43079	29	45634	1.059	152/3452
High Mountains	30103	20	15593	0.518	515/5202
High Himalayas	35353	24	15673	0.443	2150/8749

Table 3. Details on the data points across the river basin units.

River Basins	Total Area (Sq. Km.)	Area within Nepal (Sq. Km.)	Percentage of area in Nepal (%)	No. of Spot Elevation Points	Point Density (Points per Sq. Km)	Elevation Range (Min/Max) masl
Kankai	1280	1280	100	1504	1.2	76/3234
Koshi	59565	27687	46	14676	0.5	66/8586
Kamala	2007	2007	100	1507	0.8	68/2021
Bagmati	4304	4304	100	3339	0.8	71/2697
Narayani	36598	32094	88	26316	0.8	110/8167
West Rapti	6449	6444	100	8224	1.3	131/3267
Babai	3424	3424	100	5096	1.5	138/2445
Karnali	45974	42909	93	29324	0.7	137/7751
Mahakali	15460	5209	34	4669	0.9	154/7132

3.3 Methodology

The overall methodology in this study involves the use of ArcGIS, excel and python tools. The point shapefile of the spot elevation data along with the layers of physiographic and river basins divisions were imported in the ArcMap platform of ArcGIS. These points lying within each physiographic unit were separately clipped and the DEM elevation at these point locations were extracted using 'Extract Multi values to Points' tool within spatial analyst toolbox in ArcMap. This resulted in a separate elevation field for each of the DEM used, corresponding to the spot elevation points. The attributes were then exported to excel for further analysis. The same procedure was followed for the analysis at the river basin level too.

The accuracy was evaluated based on some commonly adopted statistical measurements (**Table 4**). The vertical accuracy of the eight DEMs used in this study was calculated from the differences corresponding between the elevation of the DEM pixel and the reference point spot elevation. Elevation error (the difference in elevation between DEM and spot elevation, ($\boldsymbol{Z_{Error} = Z_{DEM} - Z_{SEl}}$) was estimated where the positive error denote overestimation in DEM while the negative error denotes underestimation of DEM elevation. The mean of the reference spot elevation and the DEM elevation over each physiographic division (or river basins) was calculated as the sum of the elevation divided by the number of points. The other statistics (**Table 4**) mean error (ME), mean absolute error (MAE), root mean square error (RMSE) were calculated based on the elevation error as described above. Additionally, the coefficient of determination ($\boldsymbol{R^2}$) between spot elevation and each of the DEMs elevation was also assessed separately for each physiographic division and river basin. A histogram of the mean error of each DEM for each of the physiographic unit (and river basin) was plotted. A normal

distribution curve was fitted to the histogram. Finally based on each of the statistical measurements, the ranking of the DEMs was evaluated.

Table 4. Statistical measurement adopted for the evaluation of accuracy of DEMs.

Error Statistics	Description
Elevation Error	$Z_{error} = Z_{DEM} - Z_{SEL}$
Mean Error (ME)	$ME = \frac{\sum_{i=1}^{n} Z_{error}}{n}$
Mean Absolute Error (MAE)	$MAE = \frac{\sum_{i=1}^{n} \lvert Z_{error} \rvert}{n}$
Root Mean Square Error (RMSE)	$\sqrt{\frac{\sum_{i=1}^{n} (Z_{error(i)})^2}{n}}$

4. RESULTS AND DISCUSSION

The results for the physiographic and river basin level are discussed separately.

4.1 Evaluation across the physiographic unit

The analysis of the results across the physiographic divisions are presented herein.

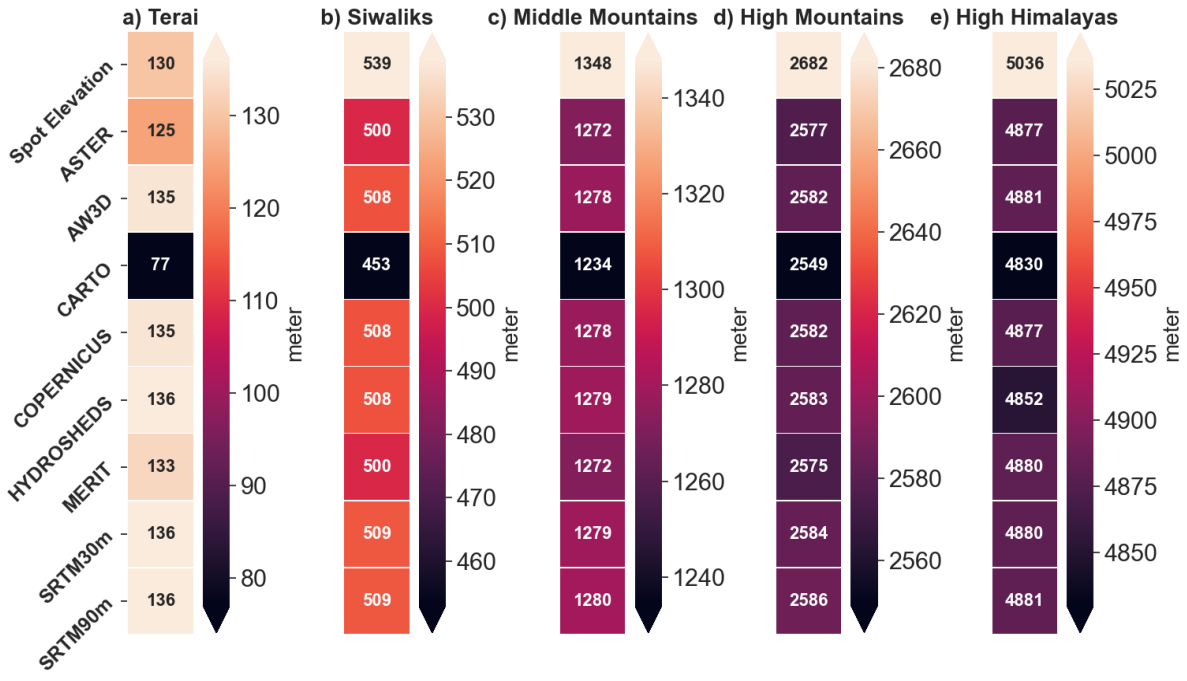

Figure 4. Comparison of the mean value of reference spot elevation data with different DEMs elevation for each physiographic unit.

The mean of the spot elevation points within each physiographic unit and the mean of the DEMs

298 elevation corresponding to these points were compared (**Figure 4a-e**). Except for the Terai, the
299 mean elevation of each of the DEMs showed underestimation across every physiographic
300 division. Carto DEM showed the maximum underestimation at every physiographic unit while
301 in Terai the ASTER DEM also displayed a slight underestimation (-5m). Apart from these, in
302 Terai, all other six DEMs exhibited overestimation ranging from +3m to +6m. MERIT DEM
303 with an overestimation of +3m depicted better performance among all others (**Figure 4a**). Terai
304 being the southern plain are the most prone to floods, sedimentation and inundation problems
305 as all the rivers from the north traverse this region. The elevation ranges also being
306 comparatively narrower in Terai due to the flat area, the accuracy of DEM is highly necessitated
307 for their application in any works related to the landuse planning and management, floods
308 management, etc. In this regard, Japan International cooperation agency (JICA) is analyzing the
309 viability of preparing a high resolution DEM of 13 districts in Terai of Province 1 and 2 and 3
310 (JICA 2020).

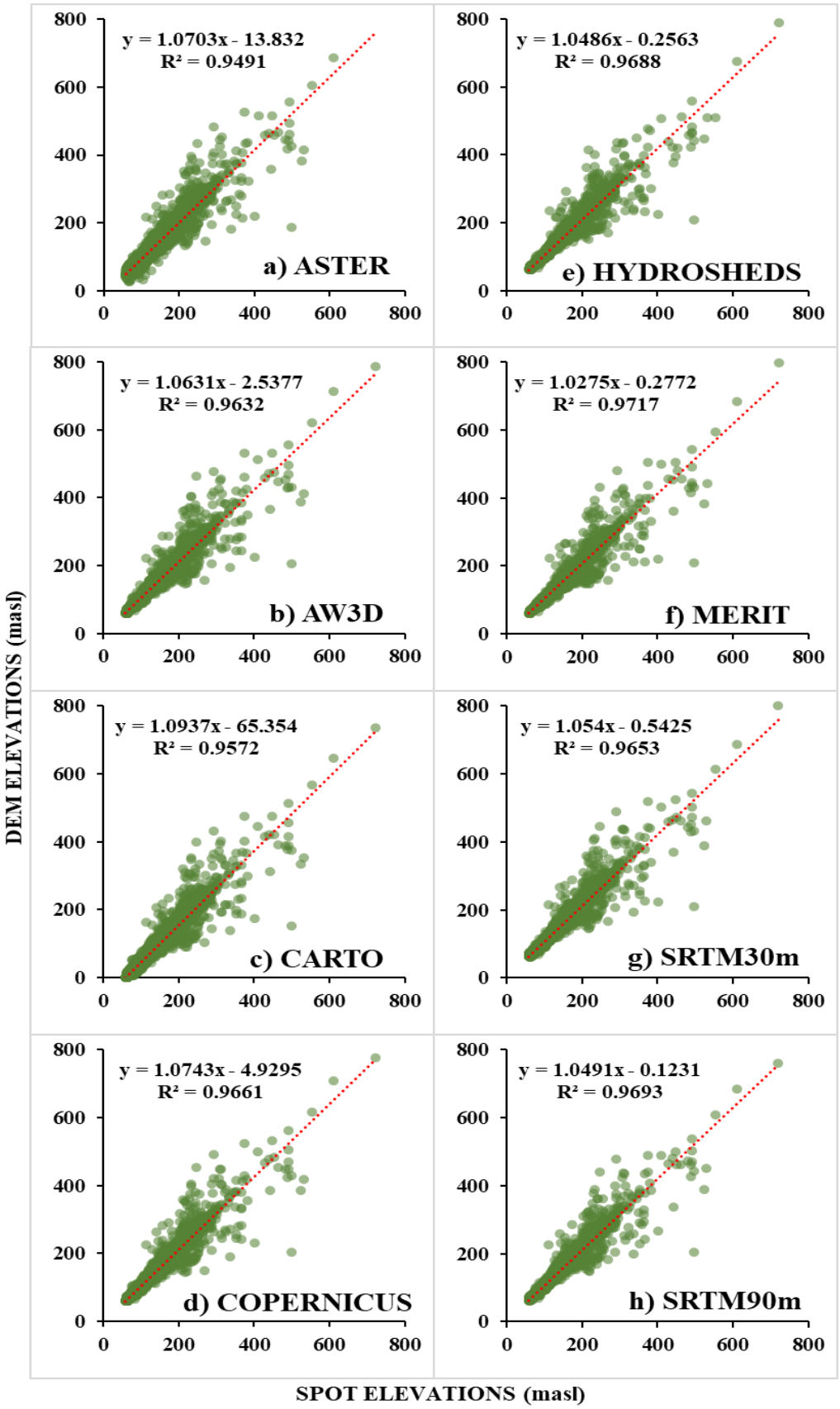

311

312 **Figure 5**. Scatterplot of reference spot elevation versus elevation of different DEMs at
313 corresponding points for the Terai region.

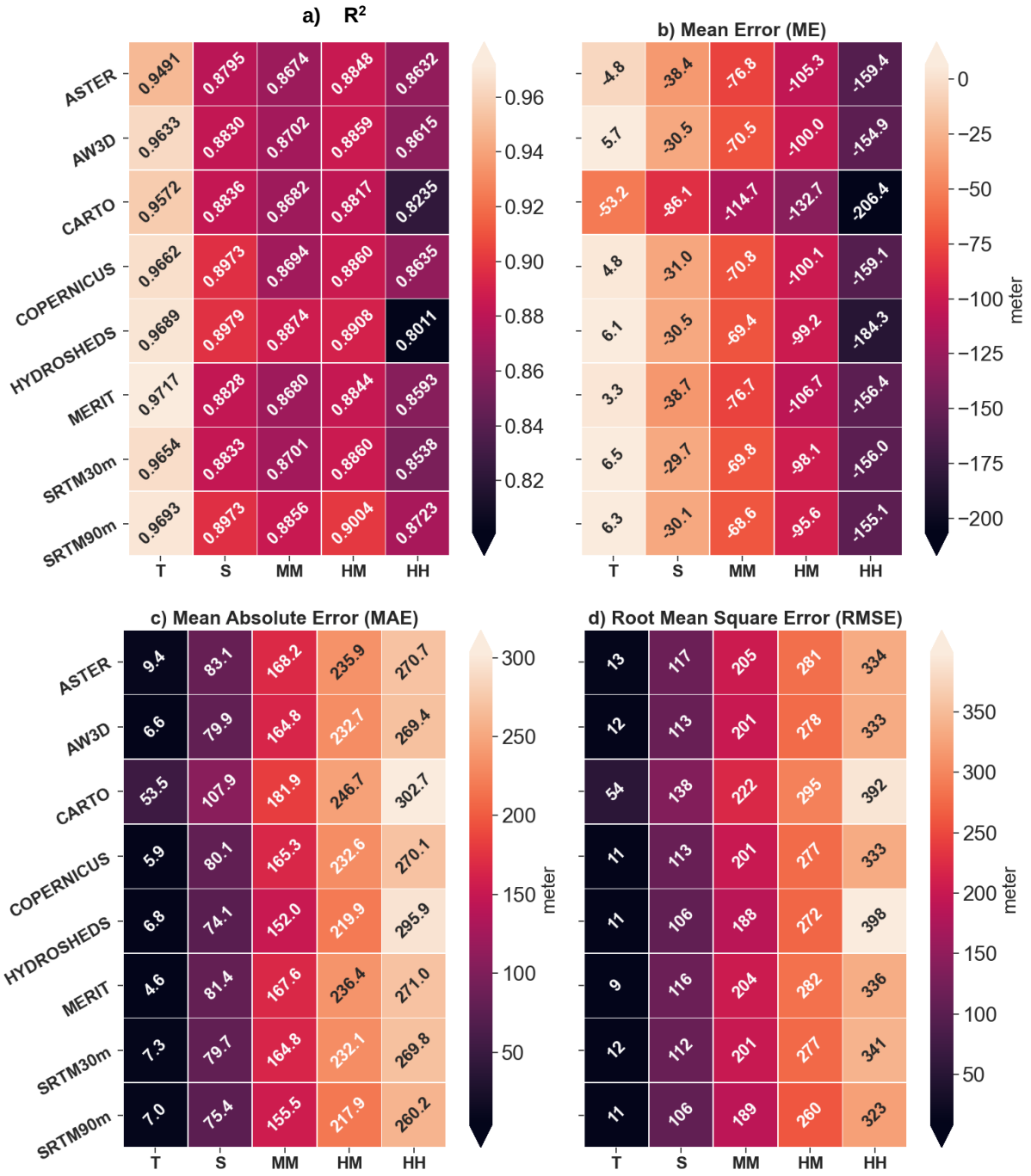

[**T**: Terai **S**: Siwalik **MM**: Middle Mountains **HM**: High Mountains **HH**: High Himalayas]

Figure 6. Comparison of different statistical measurement for each DEMs estimated from the elevation error across each physiographic unit.

The deviation of the DEMs elevation from the reference spot elevation is given by mean error (ME) in **Figure 6b**. In Siwalik region, ASTER and MERIT, showed greater deviation (both above -38m) after CARTO while the remaining SRTM30m, SRTM90m, HYDROSHEDS, COPERNICUS and AW3D showed almost similar results (error approximately between -30m to -31m) (**Figure 6b**). Except CARTO, the mean error of other DEMs for MM, HM and HH

was in the range of -68.6m to -76.8m, -95.6m to -106.7m and -154.9m to -184.3m respectively. The correlation plot between the spot elevation points and the DEMs elevation at corresponding points for the Terai region is illustrated in **Figure 5a-h**. But the coefficient of determination ($\boldsymbol{R^2}$) values between spot elevation and each DEMs across every physiographic division is depicted in **Figure 6a.** In general, the $\boldsymbol{R^2}$ values were excellent for each DEMs and across every division. Nevertheless, the values were higher (>0.9491) for Terai while for S, MM and HM, the values were very close to each other (from 0.87 to slightly above 0.90). Meanwhile, the correlation was relatively lower for High Himalayas (**Figure 6a)** which is likely due to the smaller number of elevation points with comparison to others. Likewise, MAE and RMSE are portrayed in Figure **6c-d** respectively. The values of MAE and RMSE for each DEMs across each physiographic division followed the same pattern as of mean error. Since the elevation range increases from the south to the north, the error range also followed the same pattern. Analysis by Mukherjee et al. (2012) also showed the DEM elevation to be more erroneous in high altitudinal zone where terrain is rugged.

Figure 7 and **8** illustrate the histogram of elevation errors for each DEM across different physiographic division. The normal distribution curve is fitted to the elevation errors which is represented by the bold red line in all the graphs. The histogram plot clearly shows that the negative bias is dominant in almost all of the DEMs across all physiographic division indicating underestimation of the DEMs elevation. The histogram, in general, revealed that the frequencies of negative errors are higher than the positive ones. This meant that the frequencies of the negative errors are positively skewed. However, in the case of Terai, all DEMs except ASTER and CARTO indicated the frequency of positive error to be greater than the negative ones which implied that the frequency of positive errors is negatively skewed. The mean error for these two DEMs are therefore negative (-4.8m for ASTER and -53.2m for CARTO). The histogram of AW3D, COPERNICUS, HYDROSHEDS, MERIT, SRTM30m and SRTM90m all displayed a bias toward positive values on a normal distribution and hence the mean error for these six DEMs revealed positive values in the Terai.

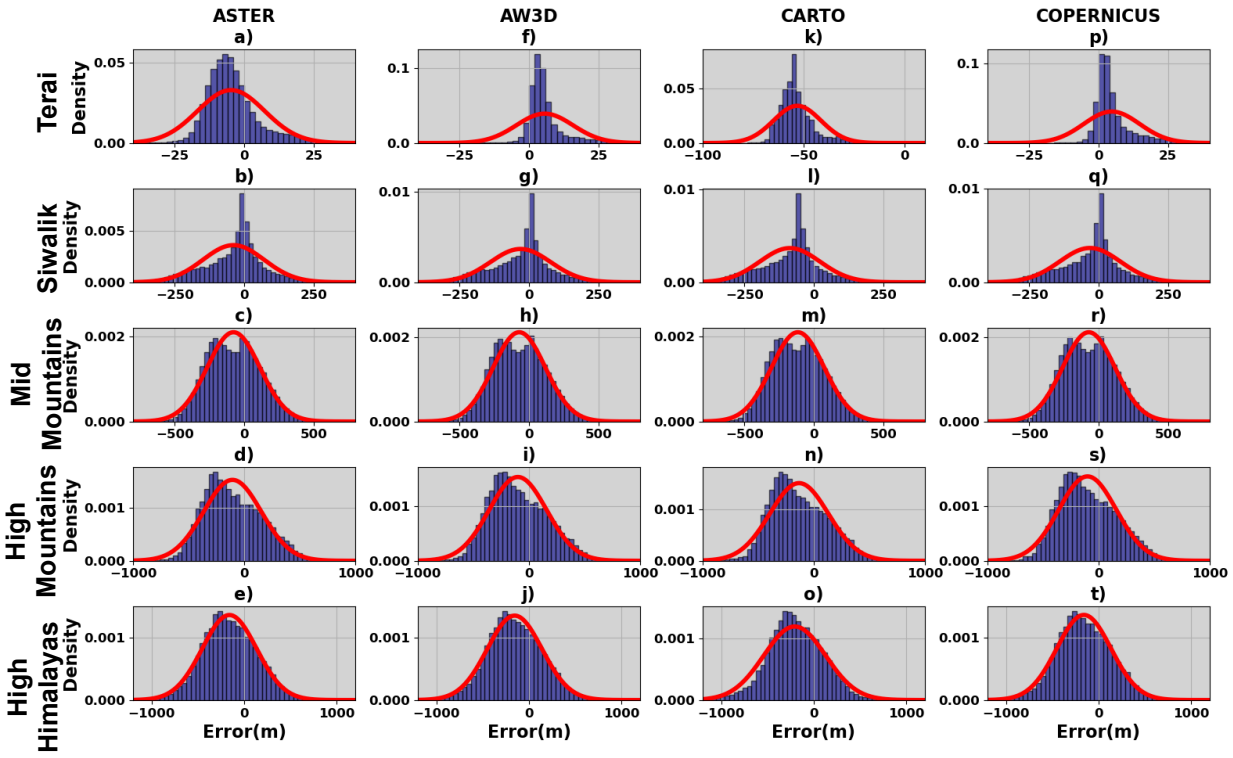

Figure 7. Histogram of elevation error for ASTER, AW3D, CARTO and COPERNICUS across each physiographic division. The red line in the figure represents the fitted curve based on normal distribution.

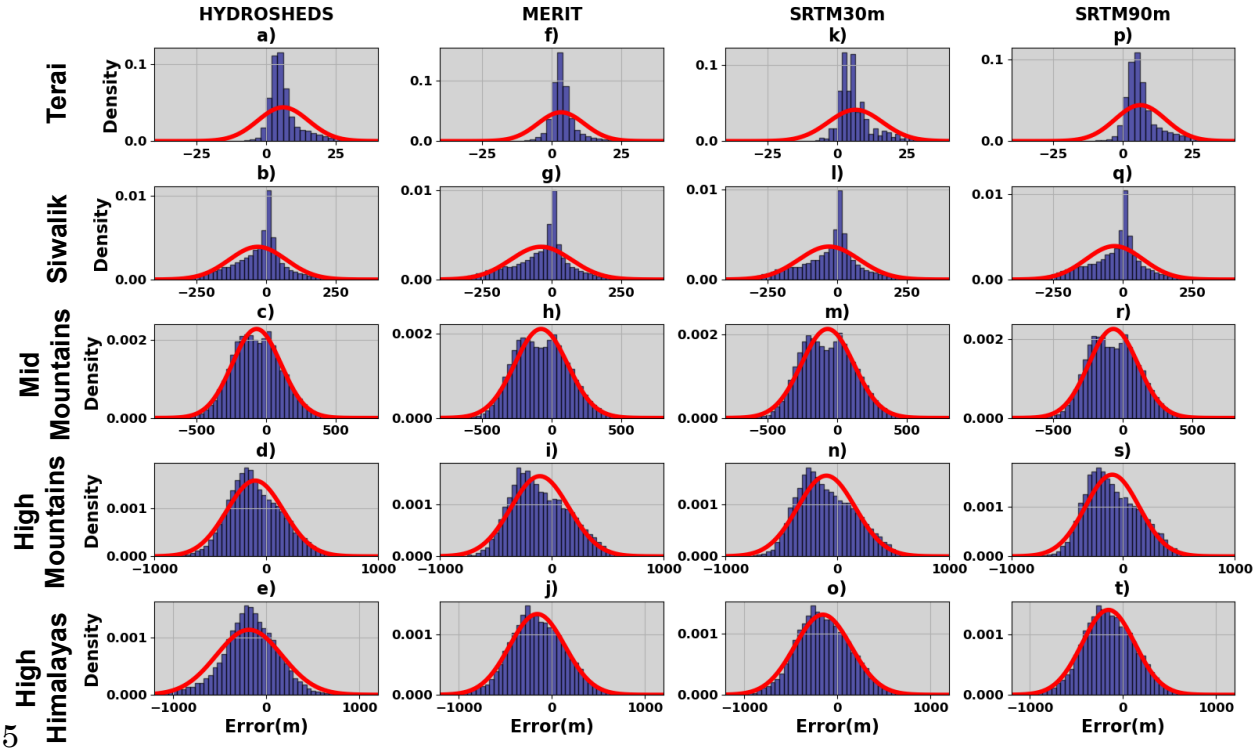

Figure 8. Histogram of elevation error for HYDROSHEDS, MERIT, SRTM30m and SRTM90m across each physiographic division. The red line in the figure represents the fitted curve based on normal distribution.

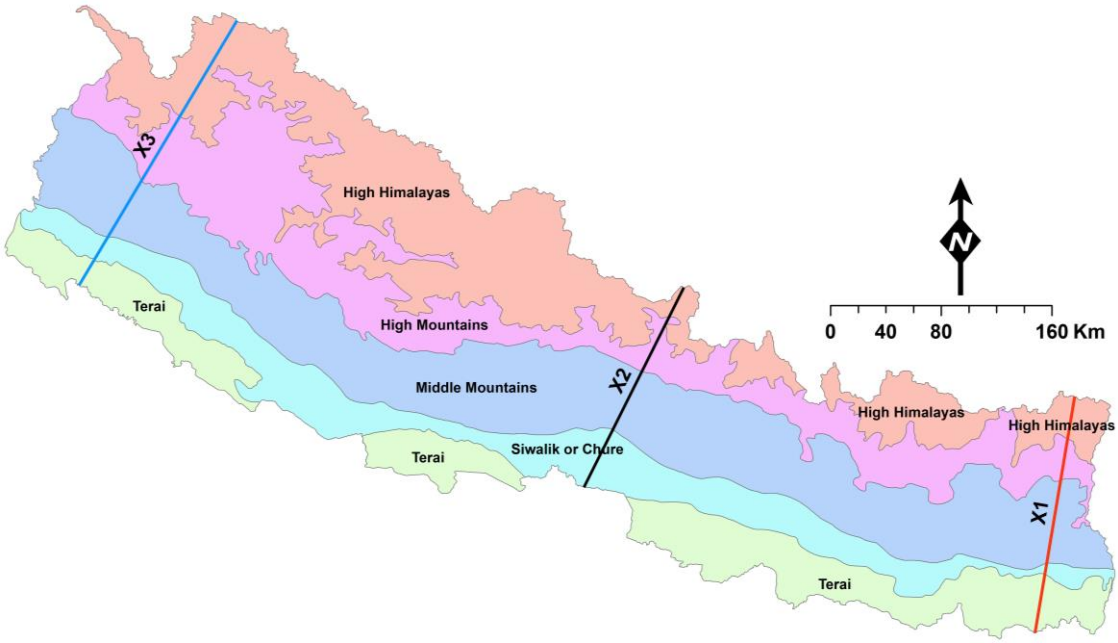

Figure 9. Physiographic Divisions with three arbitrary cross-section lines for plotting elevation profiles.

Three arbitrary cross-sections, one at the eastern part, second at the central part and the last at the western part, were drawn along the south-north direction of the country (**Figure 9**). Points were generated along these cross-section lines at an interval of 30m. DEMs elevation at these points along each cross-section are plotted against the cumulative distance (in kilometer) beginning from the south (**Figure 10a-j** and **Figure 11a-d**). In MM and HM, the elevation of each DEMs nearly matched each other (**Figure 10c-d, h-i** and **Figure 11b-c**). However, in the case of Terai, the elevation of CARTO was highly below the other DEMs showing consistent downward shift. The elevation of ASTER too was below the other DEMs but having relatively lower difference than the CARTO. The other DEMs, however, showed almost similar elevation trend. It can be observed that the elevation drops by over 150m at a distance of about 40Km at X1 (**Figure 10a**) and more than 100m at a distance of 22Km at X3 (**Figure 10f**). In Siwalik region, the elevation of CARTO was again below other DEMs particularly around the valley areas (**Figure 10b** and **11a**) while the HYDROSHEDS elevation was slightly above others around the valley of Siwalik region. At X2, the Siwalik hills form the border with India, therefore the Terai is missing in **Figure 11**.

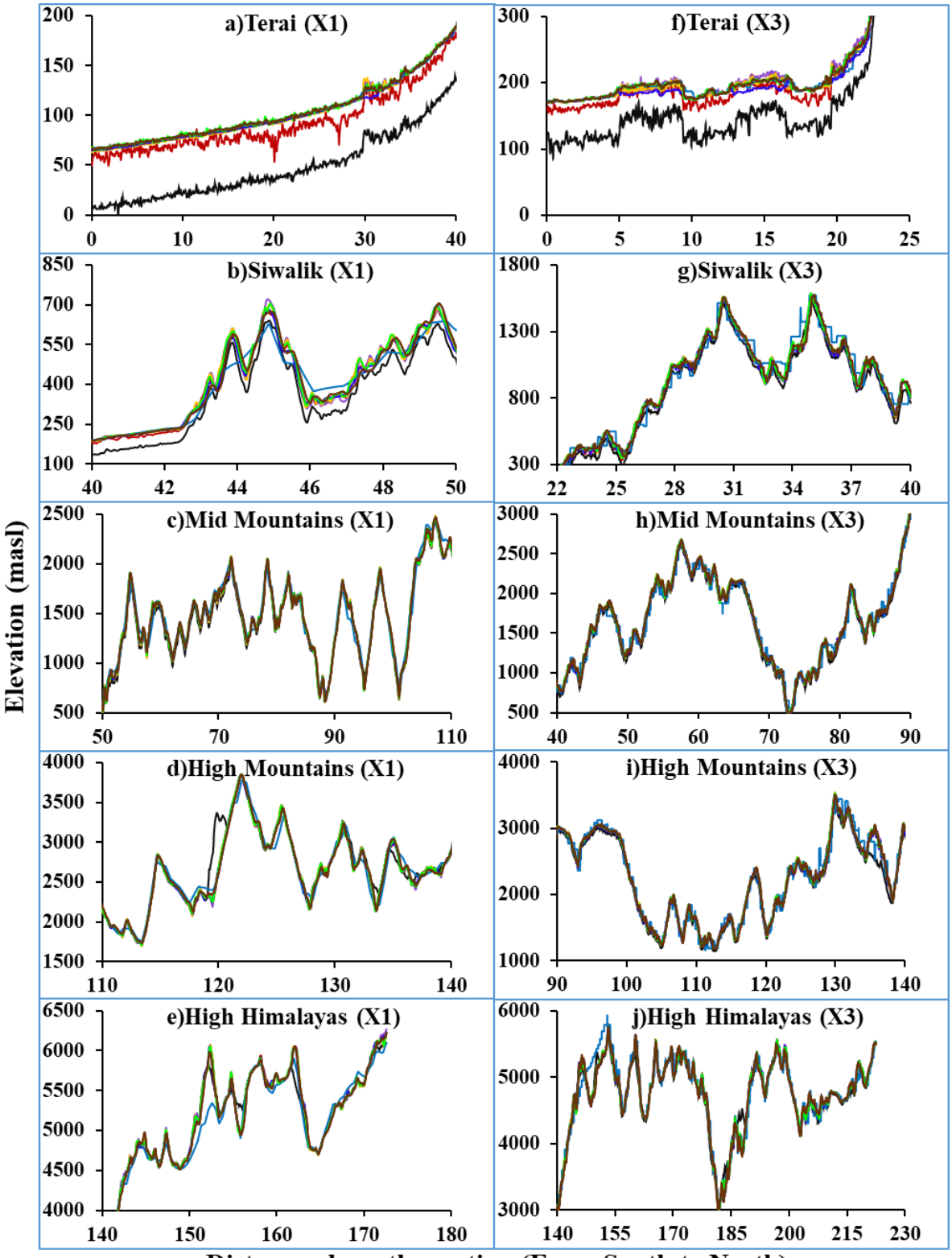

Figure 10. Elevation of different DEMs along the cross-section X1 and X3 as indicated in **Figure 9** for different physiographic division.

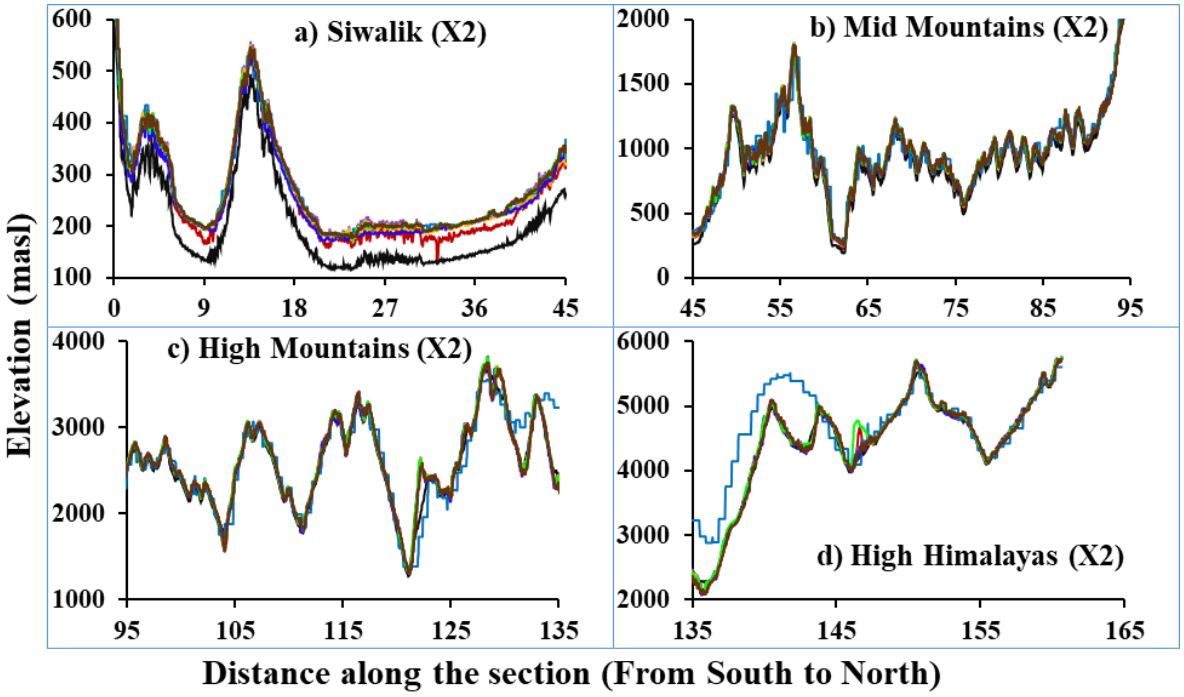

Figure 11. Elevation of different DEMs along the cross-section X2 as indicated in **Figure 9** for different physiographic division.

4.2 Evaluation across the river basins

The analysis of the accuracy of DEMs across the river basins are presented in a similar way to the analysis across the physiographic divisions

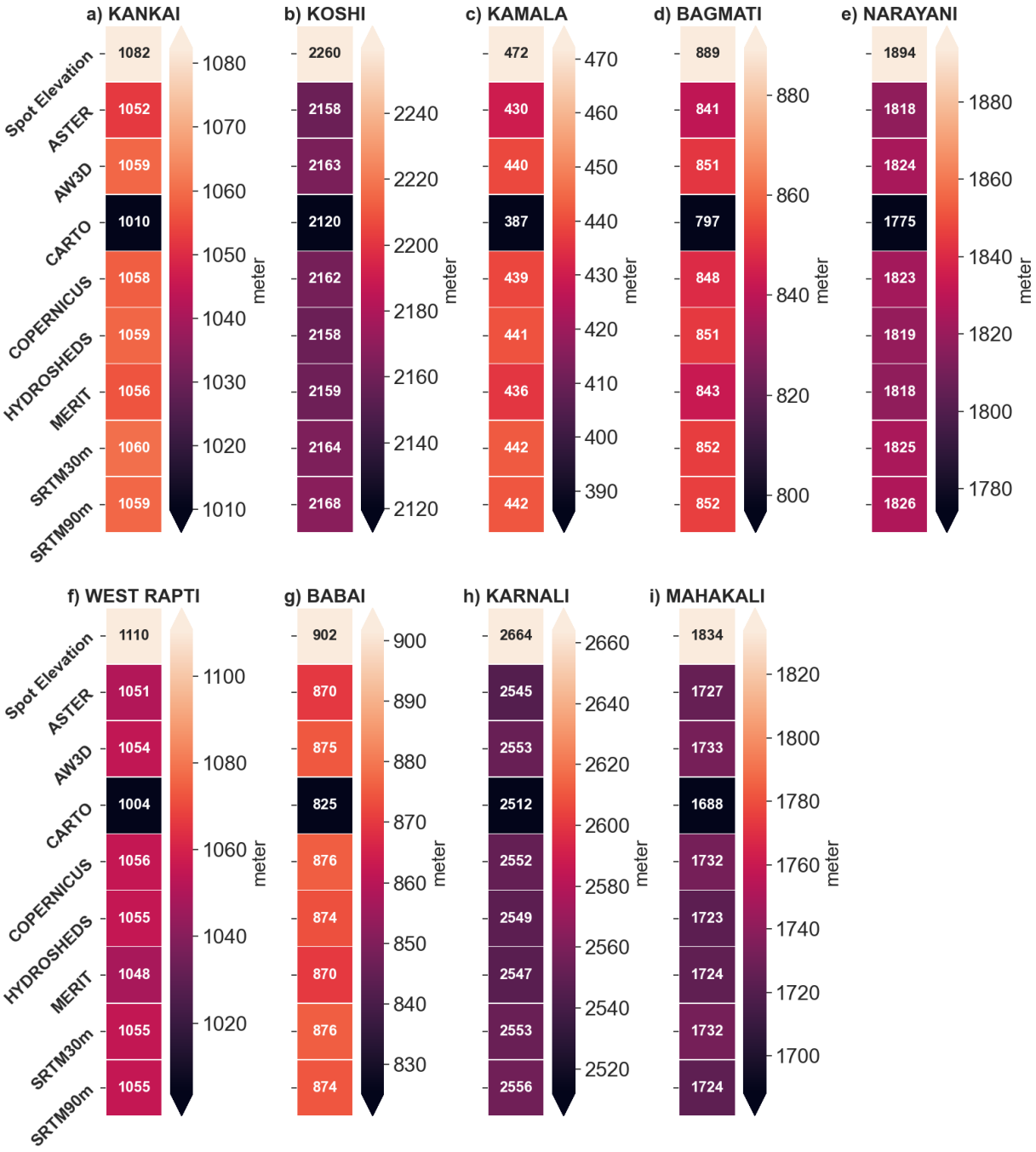

Figure 12. Comparison of the mean value of reference spot elevation data with different DEMs elevation for each river basins.

The mean of the spot elevation points within each river basin and the mean of the DEMs elevation corresponding to these points were compared (**Figure 12**). Each DEMs across all the river basins showed underestimated elevation compared to the spot elevation mean. As in the

case of physiographic divisions, CARTO displayed the maximum underestimation from the spot elevation mean in each river basins. After CARTO, the ASTER depicted greater underestimation in all basins except West Rapti and Mahakali.

The estimation of different error statistics is presented in **Figure 14a-d.** The R^2 value in general were in a good range for all the DEMs (**Figure 14a)**. Nevertheless, larger basins like Koshi, Narayani, Karnali relatively displayed higher R^2 (>0.98). In general, the elevation of SRTM90m better correlated with the spot elevation in each river basins. The correlation plot of spot elevation points versus DEMs elevation for the Koshi river basin also depicts higher R^2 (0.9846) for SRTM90m (**Figure 13)**. The range of the elevation is also higher in Koshi basin among all other river basins (**Figure 3** and **Table 3**). Meanwhile, SRTM90m also discerned the minimum mean error for four of the river basins including Koshi (-90m), Bagmati (-37m), Narayani (-68m) and Karnali (-109m) (**Figure 14b**). For other basins (Kankai, Kamala, Babai and Mahakali), SRTM30m revealed the minimum mean error (-22m, -30m, -26m and -102m respectively). Similarly, the mean error estimated for COPERNICUS was the minimum (-55m) in West Rapti basin in comparison to the other DEMs. In Mahakali basin, AW3D and COPERNICUS and in Babai, COPERNICUS also showed the same accuracy in terms of mean error as that of SRTM30m. In summary, all the DEMs exhibited negative mean error across all the river basins indicating negative bias or underestimation of the DEMs elevation. In terms of the MAE, SRTM90m outperformed other DEMs in Koshi, Narayani and Karnali While HYDROSHEDS showed better MAE in rest of the river basins (**Figure 14c**). Meanwhile, based on the RMSE, SRTM90 revealed improved performance in Koshi, Kamala, Bagmati, Narayani, West Rapti and Karnali Basins (**Figure 14d**). Similarly, in Kankai and Babai basins, HYDROSHEDS was better while SRTM30m was better in Mahakali in terms of RMSE.

The histogram of the elevation errors of the DEMs for Kankai, Kamala, Bagmati, West Rapti and Babai basins are plotted in **Figure 15** (ASTER, AW3D, CARTO and COPERNICUS) and **Figure 16** (HYDROSHEDS, MERIT, SRTM30m and SRTM90m). Similarly, **Figure 17** and **Figure 18** demonstrate the same for Koshi, Narayani, Karnali and Mahakali basins. As in the case of physiographic divisions, the histogram plot of elevation error of each DEMs depicted negative bias across all river basins. The histogram, in general, revealed that the frequencies of negative errors are higher than the positive ones. This meant that the frequencies of the negative errors are positively skewed. However, in the case of Terai, all DEMs except ASTER and CARTO indicated the frequency of positive error to be greater than the negative ones which implied that the frequency of positive errors is negatively skewed.

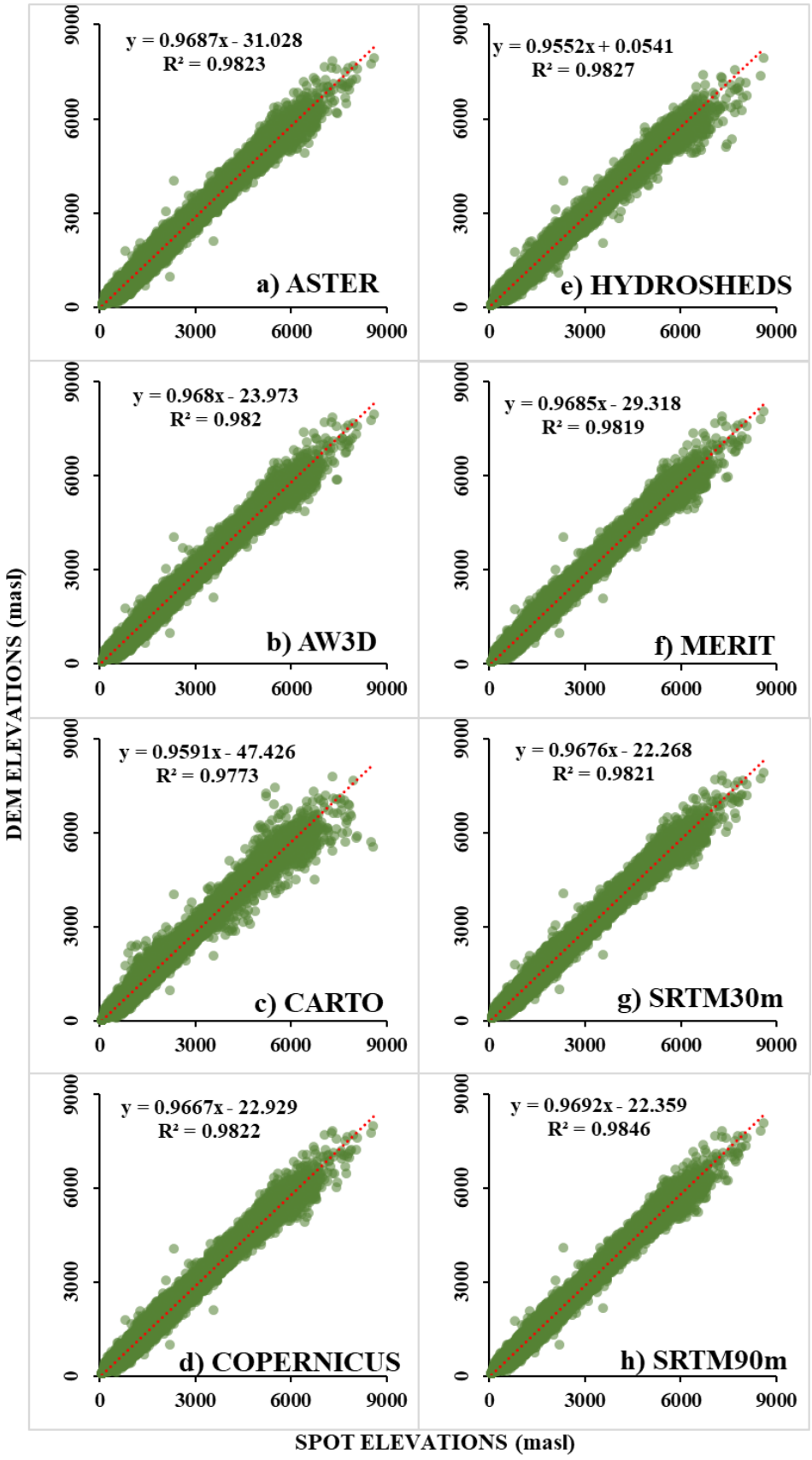

Figure 13. Scatterplot of reference spot elevation versus elevation of different DEMs at corresponding points for the Koshi River Basin.

443

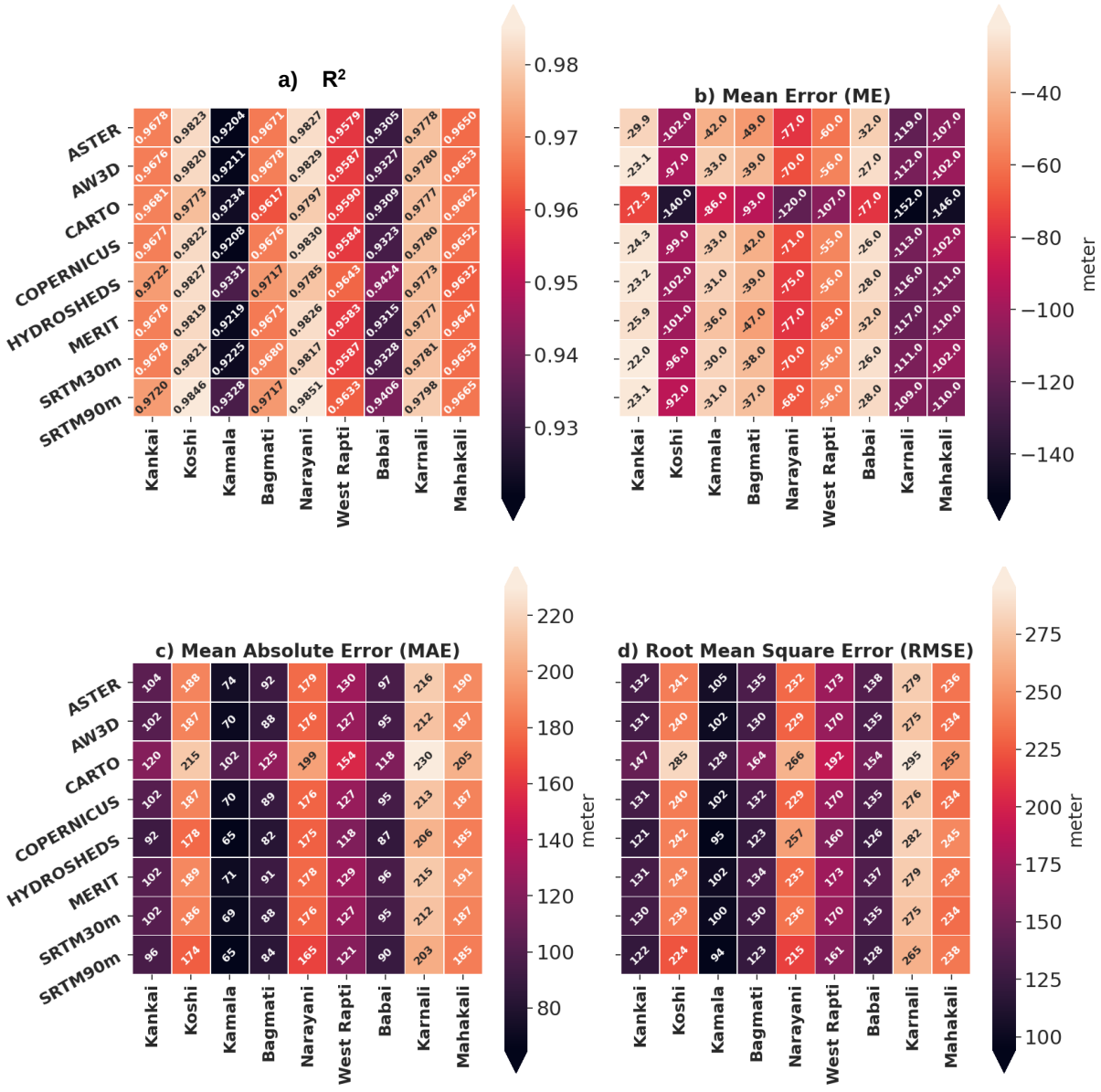

444

445 **Figure 14**. Comparison of different statistical measurements for each DEMs estimated from
446 the elevation error across each river basins.

447

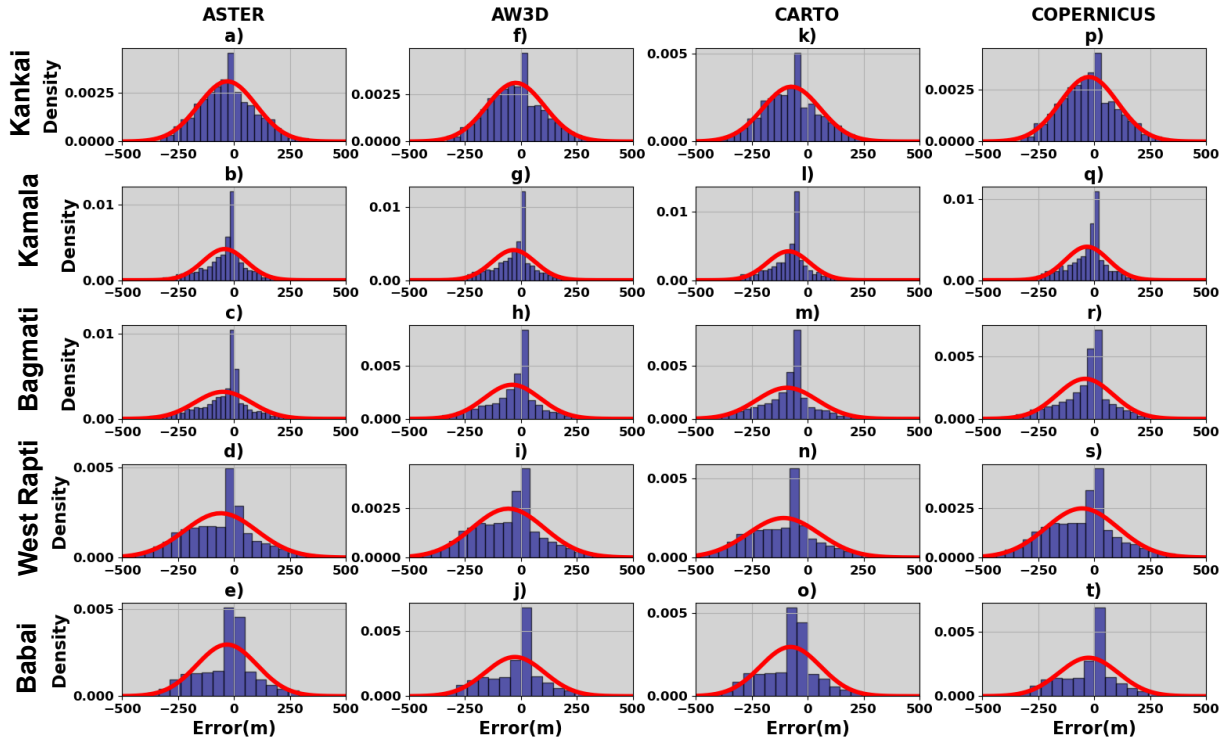

Figure 15. Histogram of elevation error for ASTER, AW3D, CARTO and COPERNICUS across five river basins. The red line in the figure represents the fitted curve based on normal distribution.

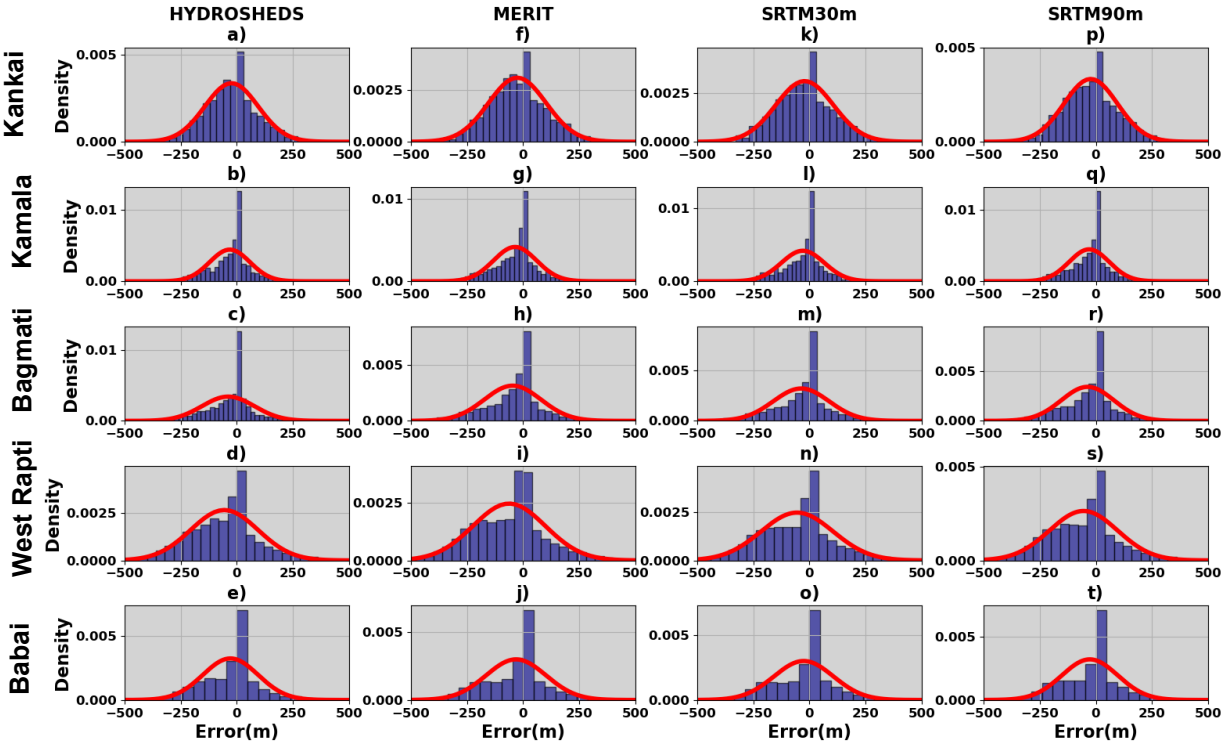

Figure 16. Histogram of elevation error for ASTER, AW3D, CARTO and COPERNICUS across five river basins. The red line in the figure represents the fitted curve based on normal distribution.

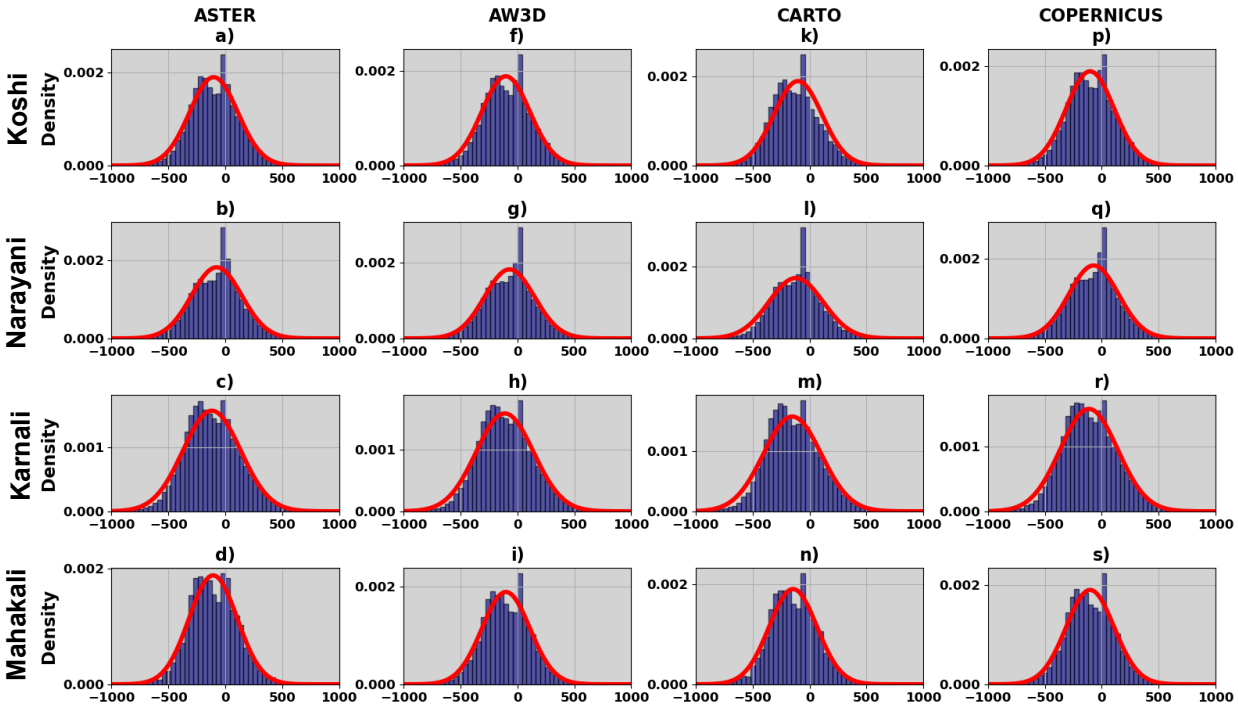

Figure 17. Histogram of elevation error for ASTER, AW3D, CARTO and COPERNICUS across four river basins. The red line in the figure represents the fitted curve based on normal distribution.

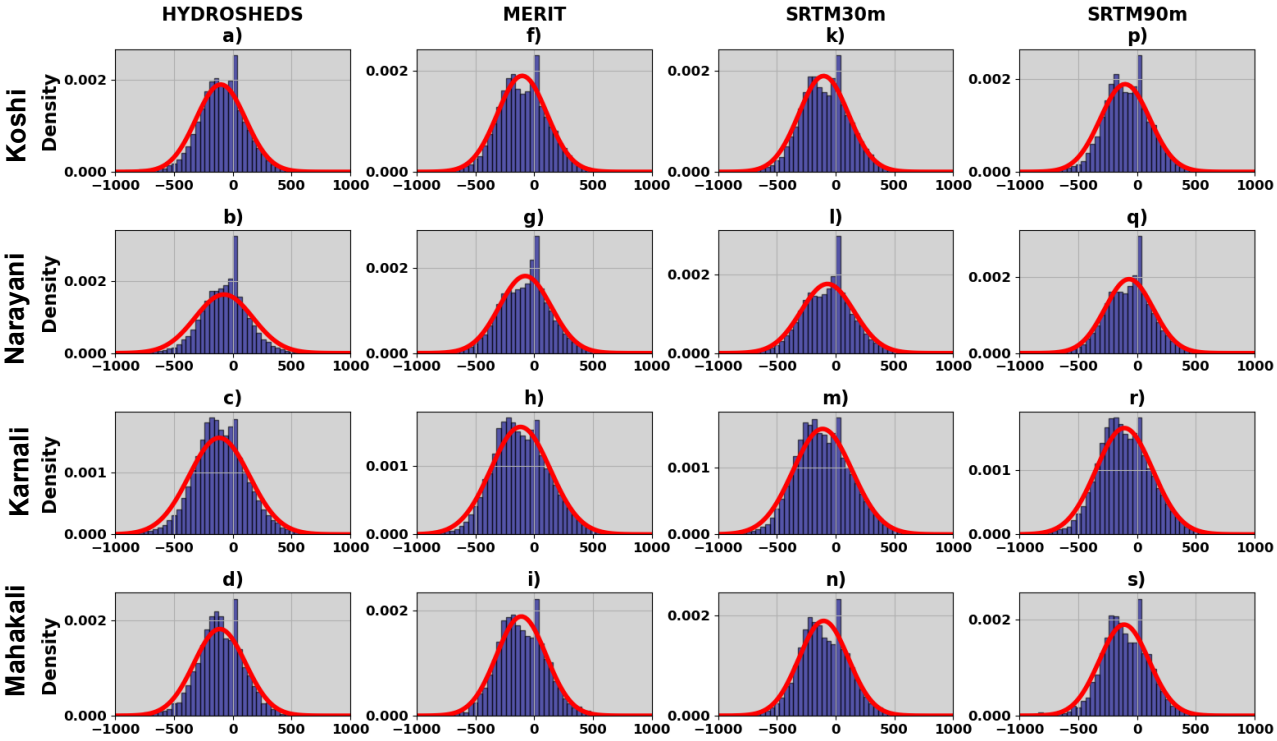

Figure 18. Histogram of elevation error for ASTER, AW3D, CARTO and COPERNICUS across four river basins. The red line in the figure represents the fitted curve based on normal distribution.

4.3 Raking of the DEMs

4.3.1 Ranking at the physiographic division

The eight DEMs considered in this study are ranked between 1 to 8 based on their values of

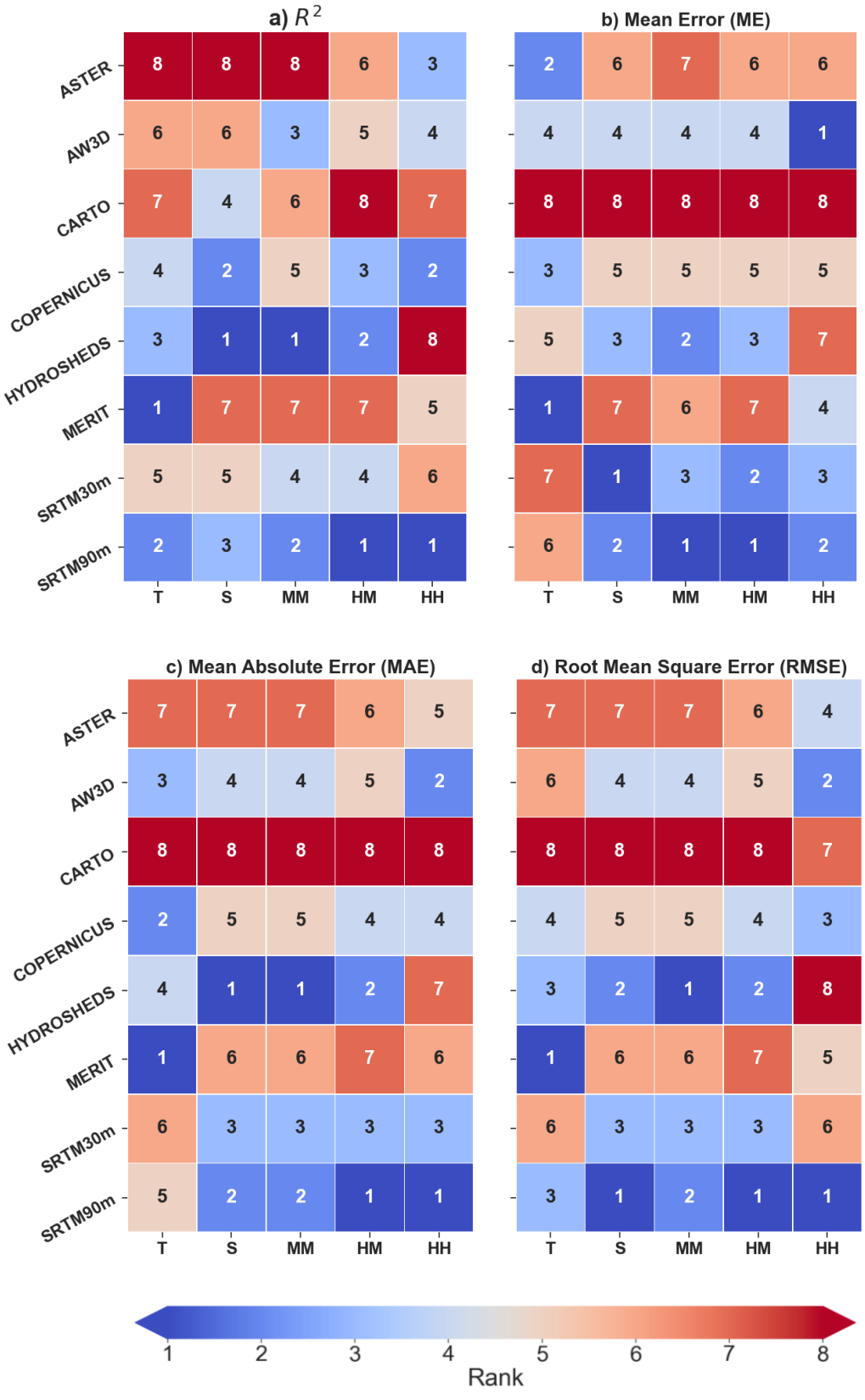

Figure 19. Ranking of the DEMs across different physiographic divisions based on the statistical measurements of the elevation error.

error statistics. The four statistical measurements of the error as presented in the previous section are R^2, ME, MAE and RMSE. The DEM with higher R^2 value is ranked 1 while the lowest one is ranked 8. For other three statistics, the DEMs showing the lowest ME, MAE and RMSE are ranked 1 while those exhibiting the highest values are ranked 8. Accordingly, **Figure 19** depicts the rank of each DEMs across different physiographic divisions.

Based on all the error statistics, for Terai, MERIT exhibited the best accuracy among all the DEMs analyzed in this study. In the case of Siwalik, SRTM90m ranked first based on RMSE while SRTM30m ranked first based on the ME. Similarly, HYDROSHEDS came first in terms of R^2 and MAE. However, the difference in error statistics values between HYDROSHEDS and SRTM90m were extremely marginal. HYDROSHEDS also ranked first in three of the four error statistics in the middle mountains. In high mountain and high Himalayas, SRTM90m proved to be superior to its other counterpart DEMs in all four statistical measurements.

4.3.2 Ranking at the river basins

As in the case of physiographic divisions, the ranking of different DEMs across different river basins are prepared based on the values of the measurement of the error statistics **(Figure 20)**.

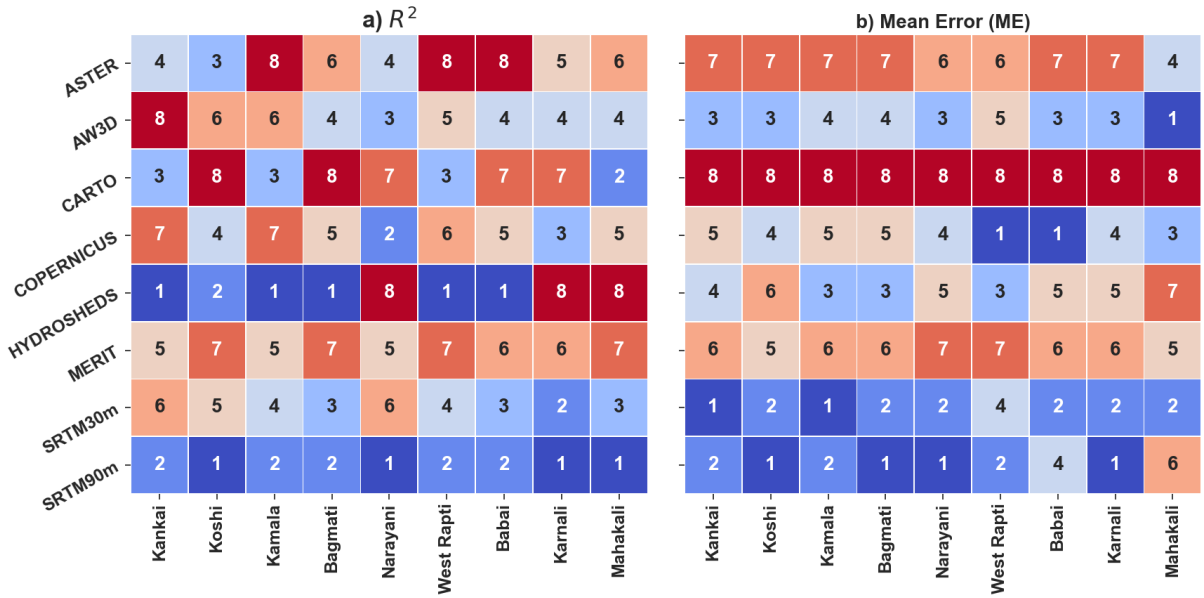

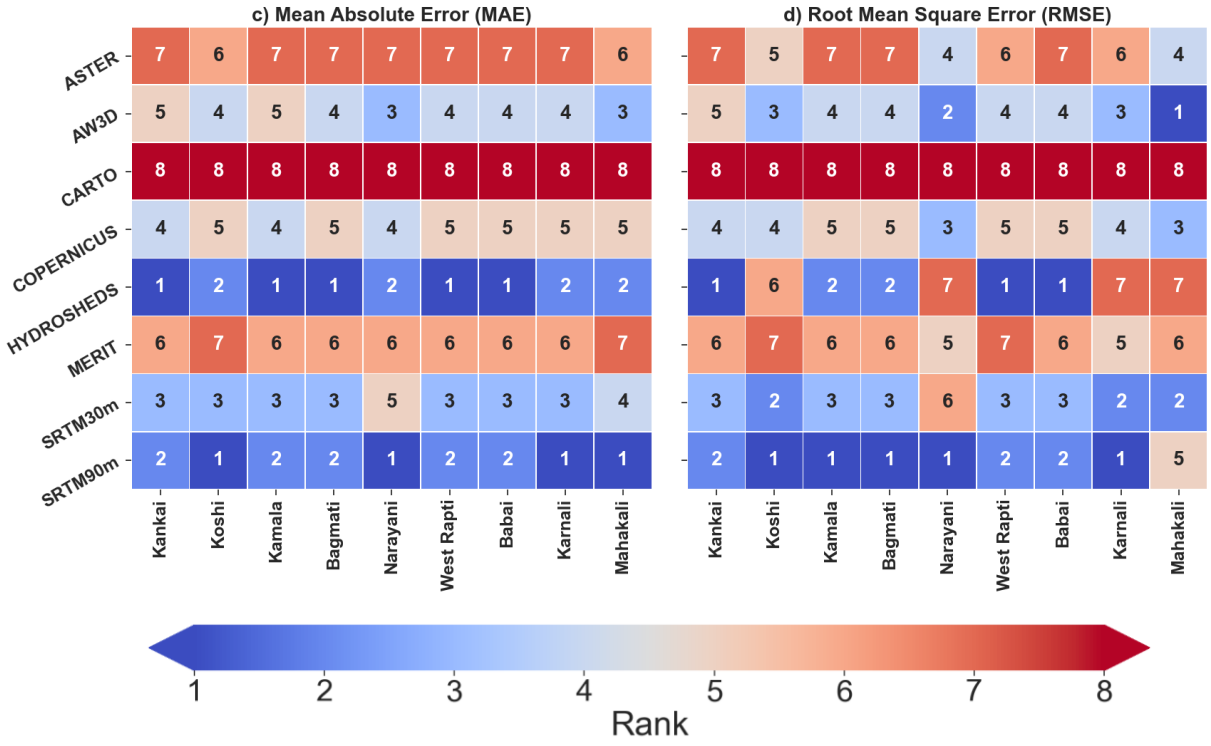

Figure 20. Ranking of the DEMs across different river basins based on the statistical measurements of the elevation error.

SRTM90m depicted better performance in most of the river basins. In terms of R^2, it ranked first in four river basins and second in five basins (**Figure 20a**). Similarly, in four basins, SRTM90m ranked first based on the ME while in three basins, it ranked second. SRTM90m also showed first rank in four basins and second rank in five basins in terms of MAE. In all the basins where SRTM90m came second, HYDROSHEDS ranked number one with a very slim margin of error. In larger basins Koshi, Narayani and Karnali, SRTM90m by ranking number one, proved its dominance over other DEMs based on all the error statistics. MERIT DEM which had shown highest accuracy in Terai region, performed poor at the river basins level. HYDROSHEDS seems to be preferrable in basins like Kankai, Kamala, Bagmati, West Rapti and Babai along with SRTM90m. While in Mahakali, AW3D showed the number one rank in terms of RMSE and ME. The issue that needs a few attentions is the performance of COPERNICUS DEM. COPERNICUS released in 2020 is a relatively new product as compared to other DEMs and their applicability is yet to be examined in hydrological or geoscience studies. It ranked number one in couple of basins like West Rapti and Babai in terms of ME. In terms of RMSE, it ranked third in Narayani and Mahakali. In this regard, it also seems to be a promising product to be tested. CARTO and ASTER were left far-behind other DEMs in all the basins.

5. CONCLUSIONS

The application of DEMs is imminent in any studies concerning the topography as it is a fundamental input data for many geoscience studies. High-resolution DEMs are considered to be a vital tool for mapping and modelling different natural hazards and risks that are influenced by topography. The availability and access to space-borne DEMs is ever increasing. The DEMs, however, are not free from errors arising from different sources during the observations. In this context, the choice of the selection of DEMs becomes a tricky issue for its user. Inaccuracy in the input topography will likely influence the results and thus deceive the users and the planners. Against this backdrop, we evaluated the vertical accuracy of eight different DEMs across different physiographic divisions and the river basins of Nepal. Our results revealed that MERIT is superior to other DEMs (RMSE 9m) in the low lying Terai plains of Nepal where the elevation range is lower. In High mountains and High Himalayas having higher elevation range, SRTM90m outperformed all its counterpart under consideration which is in alignment with the findings of the past studies. Meanwhile in Siwalik and middle mountains, SRTM90m and HYDROSHEDS exhibited almost similar RMSE indicating their compatible uses in these regions.

The accuracy assessment across different river basins discerned that the accuracy of SRTM90m was above others in larger river basins like Koshi (RMSE 224m), Narayani (RMSE 215m) and Karnali (RMSE 265m) where the range of elevation is greater. In smaller to medium sized basins like Kankai, Kamala, Bagmati, West Rapti and Babai, HYDROSHEDS could be preferrable along with SRTM90m. MERIT DEM which had shown highest accuracy in Terai region, performed poor at the river basins level. Meanwhile, CARTO and ASTER were also left far-behind in accuracy than the other DEMs across all the basins.

Funding:

No funding has been received to conduct this study.

Data Availability:

The DEMs data are freely accessible across different web-platform whose source are mentioned in the description. The spot elevation points used in this study is the property of Survey Department of Nepal and cannot be distributed.

References

Amatulli G, McInerney D, Sethi T, Strobl P, Domisch S. 2020. Geomorpho90m, empirical evaluation and accuracy assessment of global high-resolution geomorphometric layers. Sci Data. 7(1):1–18.

Baral TN. 2006. STATUS OF SURVEYING AND MAPPING IN NEPAL. In: Seventeenth United Nations Reg Cartogr Conf Asia Pacific [Internet]. Vol. 6. Bangkok: UNITED NATIONS ECONOMIC AND SOCIAL COUNCIL; p. 5–65. https://unstats.un.org/unsd/geoinfo/RCC/docs/rccap17/crp/17th_UNRCCAP_econf.97_5_CRP10.pdf

Bhang KJ, Schwartz FW, Braun A. 2007. Verification of the vertical error in C-band SRTM DEM using ICESat and Landsat-7, Otter Tail County, MN. IEEE Trans Geosci Remote Sens. 45(1):36–44.

Boreggio M, Bernard M, Gregoretti C. 2018. Evaluating the differences of gridding techniques for digital elevation models generation and their influence on the modeling of stony debris flows routing: A case study from rovina di cancia basin (North-eastern Italian alps). Front Earth Sci. 6(November).

Bricker SH, Yadav SK, M MA, Satyal Y, Dixit A, Bell R. 2014. Groundwater resilience Nepal: preliminary findings from a case study in the Middle Hills [Internet]. [place unknown]. http://earthwise.bgs.ac.uk/index.php/OR/14/069_Study_area

Chhatkuli RR. 2003. Building Spatial Database for NGII in Nepal. Natl Geogr Mag [Internet].:1–11. https://citeseerx.ist.psu.edu/viewdoc/download?doi=10.1.1.210.4440&rep=rep1&type=pdf

Chu T, Lindenschmidt K-E. 2017. Comparison and Validation of Digital Elevation Models Derived from InSAR for a Flat Inland Delta in the High Latitudes of Northern Canada. Can J Remote Sens [Internet]. 43(2):109–123. https://www.tandfonline.com/doi/full/10.1080/07038992.2017.1286936

Coulthard TJ, Neal JC, Bates PD, Ramirez J, de Almeida GAM, Hancock GR. 2013. Integrating the LISFLOOD-FP 2D hydrodynamic model with the CAESAR model: Implications for modelling landscape evolution. Earth Surf Process Landforms. 38(15):1897–1906.

Dhital MR. 2015. Geology of the Nepal Himalaya [Internet]. Cham: Springer International Publishing. http://link.springer.com/10.1007/978-3-319-02496-7

DoS N. 2021. Survey Department of Nepal [Internet]. http://dos.gov.np/

DoWRI. 2019. Irrigation Master Plan. Dep Water Resour Irrig.(November).

Farr TG, Rosen PA, Caro E, Crippen R, Duren R, Hensley S, Kobrick M, Paller M, Rodriguez E, Roth L, et al. 2007. The Need for Global Topography. Rev Geophys [Internet]. 45(2):1–43. http://www2.jpl.nasa.gov/srtm/SRTM_paper.pdf

Gesch D, Oimoen M, Danielson J, Meyer D. 2016. Validation of the ASTER global digital elevation model version 3 over the Conterminous United States. Int Arch Photogramm Remote Sens Spat Inf Sci - ISPRS Arch. 41(July):143–148.

Hagen T. 1969. Report on the geological survey of Nepal. Volume 1: Preliminary Reconnaissance. [place unknown].

JAXA. 2017. ALOS Global Digital Surface Model (DSM) " ALOS World 3D-30m " (AW3D30) Dataset Product Format Description Earth Observation Research Center (EORC), Japan Aerospace Exploration Agency (JAXA). (March):11.

JICA. 2020. THE PREPARATORY SURVEY REPORT FOR THE PROJECT FOR THE DEVELOPMENT OF DIGITAL ELEVATION MODEL AND ORTHOPHOTO IN THE FEDERAL DEMOCRATIC REPUBLIC OF NEPAL [Internet]. [place unknown]. https://openjicareport.jica.go.jp/pdf/12356085.pdf

Jing C, Shortridge A, Lin S, Wu J. 2014. Comparison and validation of SRTM and ASTER GDEM for a subtropical landscape in Southeastern China. Int J Digit Earth. 7(12):969–992.

Lehner B, Verdin K, Jarvis A. 2013. HydroSHEDS Technical Documentation Version 1.2. EOS Trans [Internet]. 89(10):26. http://www.hydrosheds.org

Leister-Taylor V. 2020. Copernicus DEM Copernicus Digital Elevation Model Validation Report [Internet]. [place unknown]. https://spacedata.copernicus.eu/documents/20126/0/GEO1988-CopernicusDEM-RP-001_ValidationReport_I3.0.pdf/996b90c4-49b1-0883-5553-4e29a29c4bd5?t=1609340156005

Ling F, Zhang QW, Wang C. 2005. Comparison of SRTM data with other DEM sources in hydrological researches. Proceedings, 31st Int Symp Remote Sens Environ ISRSE 2005 Glob Monit Sustain Secur.

Mukherjee Sandip, Joshi PK, Mukherjee Samadrita, Ghosh A, Garg RD, Mukhopadhyay A. 2012. Evaluation of vertical accuracy of open source Digital Elevation Model (DEM). Int J Appl Earth Obs Geoinf [Internet]. 21(1):205–217. http://dx.doi.org/10.1016/j.jag.2012.09.004

Nadi S, Shojaei D, Ghiasi Y. 2020. Accuracy Assessment of DEMs in Different Topographic Complexity Based on an Optimum Number of GCP Formulation and Error Propagation Analysis. J Surv Eng. 146(1):04019019.

NASA J. 2013. NASA Shuttle Radar Topography Mission Global 1 arc second. 2013, distributed by NASA EOSDIS Land Processes DAAC [Internet]. [accessed 2021 May 23].

614 https://doi.org/10.5067/MEaSUREs/SRTM/SRTMGL1.003
615 Nikolakopoulos KG. 2020. Accuracy assessment of ALOS AW3D30 DSM and comparison to
616 ALOS PRISM DSM created with classical photogrammetric techniques. Eur J Remote Sens
617 [Internet]. 53(sup2):39–52. https://doi.org/10.1080/22797254.2020.1774424
618 Pakoksung K, Takagi M. 2016. Digital elevation models on accuracy validation and bias
619 correction in vertical. Model Earth Syst Environ [Internet]. 2(1):11.
620 http://link.springer.com/10.1007/s40808-015-0069-3
621 Pakoksung K, Takagi M. 2020. Effect of DEM sources on distributed hydrological model to
622 results of runoff and inundation area. Model Earth Syst Environ [Internet]. 30(0123456789).
623 https://doi.org/10.1007/s40808-020-00914-7
624 Purinton B, Bookhagen B. 2017. Validation of digital elevation models (DEMs) and comparison
625 of geomorphic metrics on the southern Central Andean Plateau. Earth Surf Dyn. 5(2):211–237.
626 Rawat KS, Mishra AK, Sehgal VK, Ahmed N, Tripathi VK. 2013. Comparative evaluation of
627 horizontal accuracy of elevations of selected ground control points from ASTER and SRTM
628 DEM with respect to CARTOSAT-1 DEM: a case study of Shahjahanpur district, Uttar Pradesh,
629 India. Geocarto Int. 28(5):439–452.
630 Sampson CC, Smith AM, Bates PD, Neal JC, Trigg MA. 2016. Perspectives on open access
631 high resolution digital elevation models to produce global flood hazard layers. Front Earth Sci.
632 3(January):1–6.
633 Schumann GJ-P, Bates PD, Hawker L, Neal J, Bates PD, Elkhrachy I, Jha R, Purinton B,
634 Bookhagen B, Boreggio M, et al. 2018. The Need for a High-Accuracy, Open-Access Global
635 DEM. Front Earth Sci [Internet]. 6(1):1–5. http://dx.doi.org/10.1016/j.jag.2012.09.004
636 Sharma CK. 1987. River Systems of Nepal. [place unknown].
637 Shrestha BB. 2019. Approach for Analysis of Land-Cover Changes and Their Impact on
638 Flooding Regime. Quaternary. 2(3):27.
639 SRTM. 2015. The Shuttle Radar Topography Mission (SRTM) Collection User Guide
640 [Internet]. :1–17. https://lpdaac.usgs.gov/documents/179/SRTM_User_Guide_V3.pdf
641 Takaku J, Tadono T, Tsutsui K, Ichikawa M. 2016. Validation of “Aw3D” Global Dsm
642 Generated From Alos Prism. ISPRS Ann Photogramm Remote Sens Spat Inf Sci. III–
643 4(July):25–31.
644 Toutin T. 2008. ASTER DEMs for geomatic and geoscientific applications: A review. Int J
645 Remote Sens. 29(7):1855–1875.
646 Upreti BN. 2001. The physiography and geology of Nepal and their bearing on the landslide
647 problem. In: Landslide Hazard Mitig Hindu Kush-Himalayas [Internet]. [place unknown]:

ICIMOD. https://lib.icimod.org/record/21555/files/c_attachment_96_777.pdf

Winchell M, Srinivasan R, Di Luzio M, Arnold J. 2013. ArcSWAT Interface For SWAT2012: User's Guide. Texas Agric Exp Stn United States Dep Agric Temple, TX.:464.

Yamazaki D, Ikeshima D, Sosa J, Bates PD, Allen GH, Pavelsky TM. 2019. MERIT Hydro: A High-Resolution Global Hydrography Map Based on Latest Topography Dataset. Water Resour Res. 55(6):5053–5073.

Yamazaki D, Ikeshima D, Tawatari R, Yamaguchi T, O'Loughlin F, Neal JC, Sampson CC, Kanae S, Bates PD. 2017. A high-accuracy map of global terrain elevations. Geophys Res Lett [Internet]. 44(11):5844–5853. http://doi.wiley.com/10.1002/2017GL072874

Yan D, Wang K, Qin T, Weng B, Wang H, Bi W, Li X, Li M, Lv Z, Liu F, et al. 2019. A data set of global river networks and corresponding water resources zones divisions. Sci Data. 6(1).